Central nucleus of the amygdala to medial prefrontal cortex 5-HTergic neural circuit modulates the recovery of consciousness during sevoflurane anesthesia

YuLing Wang[1#], Yue Yang[1#], YaXuan Wu[1#], XiaoXia Xu[3#], Qing Xu[2], ZiWen Zhang[1], XuanYi Di[1], HongHai Zhang[*1,2,3]

[1]Department of Anesthesiology, the Fourth Clinical School of Medicine, Zhejiang Chinese Medical University, Hangzhou, 310006, China

[2]Department of Anesthesiology, Affiliated Hangzhou First People's Hospital, Zhejiang University School of Medicine, Hangzhou, 310006, China

3Department of Anesthesiology, Affiliated Hangzhou First People's Hospital, Westlake University School of Medicine, Hangzhou, 310006, China.

[#]These authors contributed equally to this work

[*]Corresponding authors: HongHai Zhang

Email address: zhanghonghai_0902@163.com

ORCID: http://orcid.org/0000-0003-3530-2060

Abstract

General anesthesia, widely employed for its capacity to induce unconsciousness during surgical and diagnostic procedures, frequently results in postoperative recovery delays, a common complication. The precise mechanisms underpinning this delayed emergence from anesthesia remain not fully understood. Prior research has established a strong association between sleep-wake neural circuits and the anesthetic effects of general anesthetics, with serotonin (5-HT) playing a pivotal role in the regulation of anesthesia emergence. Extensive projections exist between the amygdala and the medial prefrontal cortex (mPFC). In this study, we utilized pharmacological, chemogenetic, and optogenetic techniques to explore the relationship between the 5-HT neural circuitry within the central amygdala (CeA)-mPFC pathway and the process of awakening from general anesthesia. Our findings reveal that modulating the 5-HT system in both the CeA and mPFC, via endogenous and exogenous means, can effectively reverse delayed emergence. This suggests that the 5-HT-ergic pathway within the CeA-mPFC circuit is instrumental in regulating the awakening process from sevoflurane anesthesia. These insights may inform future clinical interventions designed to prevent delayed emergence and reduce postoperative risks.

Keywords: General anesthesia, Sevoflurane, 5-hydroxytryptamine, Central amygdala nucleus, Medial prefrontal cortex, Consciousness

1 Introduction

General anesthesia is a meticulously calibrated, drug-induced state of controlled unconsciousness that is integral to ensuring the comfort and safety of patients during surgical procedures and other invasive medical treatments[1]. Among the myriad anesthetics available, sevoflurane, a potent inhaled anesthetic, has emerged as a cornerstone in modern surgical practice due to its rapid induction and smooth recovery profile[2]. While sevoflurane is widely utilized, the exact mechanisms by which it exerts its influence on the brain, particularly its intricate role in facilitating arousal from anesthesia, remain shrouded in a degree of mystery[3,4]. Notably, delayed recovery has also become a common complication of general anesthesia[5]. Yet, instances where patients fail to regain consciousness promptly following general anesthesia can have profoundly deleterious consequences, with the most severe potentially

endangering their very lives[6–9]. Identifying and addressing the factors contributing to prolonged recovery times is therefore of paramount importance. Only through a meticulous exploration of these factors and the implementation of targeted interventions can we hope to mitigate the risks associated with delayed emergence from anesthesia, thereby enhancing overall patient safety and reducing the incidence of adverse medical events[10,11].

5-Hydroxytryptamine (5-HT), commonly referred to as serotonin, is a crucial monoamine neurotransmitter ubiquitously present in mammalian tissues[12,13]. Its role extends to numerous facets of central nervous system function, including cognitive processing, emotional regulation, sexual activity, thermoregulatory processes, and even the regulation of food consumption. Research has uncovered that during anesthesia, there are dynamic fluctuations in the levels of central 5-HT, hinting at its pivotal role in mediating the effects of anesthesia across the body[14,15]. Building upon this insight, it stands to reason that 5-HT neurons could be instrumental in the post-anesthetic recovery phase. The cerebral cortex and the dorsal raphe nucleus (DRN) boast a significant concentration of 5-HT neurons. Neurons emanating from the DRN extend widely to regions such as the midbrain and forebrain, contributing to the establishment of the ascending arousal system[16,17]. Meanwhile, the cerebral cortex, limbic system, basal forebrain, amygdala, and other nuclei rich in cholinergic and monoaminergic properties also project back to the DRN, creating a sophisticated network that orchestrates the intricate balance between sleep and wakefulness[18–20]. The central amygdala (CeA) plays a crucial role in various behaviors, including those related to fear, anxiety, and depression[21,22]. It receives an extensive array of inputs from the cerebral cortex and subcortical areas, and in turn, projects to key brainstem and diencephalic structures, as well as to regions engaged in hormonal, autonomic, and stress-related responses, thereby influencing the sleep-wake cycle[22]. Additionally, CeA also sends numerous projections to areas involved in arousal and REM (rapid eye movement) sleep, such as the PGO (pons-geniculate-occipital) waves, and to the pontine- geniculate-occipital waves, further underscoring its integral role in regulating sleep and wakefulness[23,24].

The medial prefrontal cortex (mPFC) is intricately connected with arousal-related nuclei, including the locus coeruleus and the dorsal raphe nucleus, signifying its integral role in the neural circuitry governing arousal[5,25]. This structural and functional entanglement indicates

that the mPFC is pivotal in the regulation of consciousness levels, not only during anesthesia but also during the transition from anesthesia to wakefulness[26–28]. Recent research has demonstrated that inhibiting neurons in the mPFC can delay the process of regaining consciousness after whole-body anesthesia, further reinforcing the mPFC's position as a key regulator of arousal and consciousness[29]. Additionally, studies have observed a decrease in serotonin levels in the frontal cortex during anesthesia, which may contribute to the altered state of consciousness associated with this condition. Research has revealed that the amygdala and the medial prefrontal cortex exhibit extensive neural projections to each other, yet the role of the 5-HT neuronal pathway within the CeA-mPFC circuit during the process of awakening from general anesthesia remains unclear[30,31]. Therefore, this study aims to investigate the function of 5-HT neurons in the CeA and mPFC during the induction of anesthesia with sevoflurane and the recovery process, as well as to explore the regulatory role of the 5-HT-ergic pathway within the CeA-mPFC circuit during the awakening from sevoflurane anesthesia.

In this study, we examined the impact of exogenous 5-HT administration and endogenous modulation of CeA/mPFC 5-HT neurons on sevoflurane anesthesia recovery time. Employing a multidisciplinary approach, we delineated the neurocircuitry and physiological functions between CeA and mPFC. Our findings suggest that the CeA-mPFC 5-HT circuitry regulates sevoflurane anesthesia recovery, offering insights into managing excessive sedation and delayed emergence, with potential implications for improving postoperative outcomes.

2 Materials and methods

2.1 Animals

This study was approved by the Animal Advisory Committee of Zhejiang University, and all experimental procedures adhered to the National Institutes of Health Guidelines for the Care and Use of Laboratory Animals. Wild-type C57BL/6 J mice were obtained from the Animal Experiment Center of Zhejiang University. The mice were housed and bred in the SPF-class housing facility of the Animal Center at the School of Medicine, Zhejiang University, and maintained under standard conditions (indoor temperature 25 ° C, ambient humidity 65%, 12-h light/dark cycle) with ad libitum access to rodent food and water. To eliminate potential interference from gender and the female estrous cycle, only male mice

were utilized, and all experiments were conducted between 9:00 and 15:00.

2.2 Sevoflurane anesthesia modeling and method of anesthesia induction and emergence time observation

The 8-week-old C57BL/6J mice were placed in an airtight inhalation anesthesia box (length: 20 cm, width: 10 cm, height: 15 cm; V101, RWD Life Sciences, Inc., Shenzhen, China) for 30 min before the experiment to make them adapt to the experimental environment. At both ends of the top of the anesthesia box, one end is connected to the gas input pipeline with a gas flow rate of 2L/min, while the other end is connected to the gas recovery device. A cotton pad was laid on the inner bottom of the box, and the bottom of the anesthesia box was preheated with an electric heating pad for 15 min to keep the temperature in the anesthesia box suitable and constant during the experiment. Immediately after the start of the experiment, the sevoflurane vaporizer was activated to maintain a sevoflurane vapor concentration of 3%. After 30 min of adaptation, the gas concentration of the sevoflurane volatilization tank was adjusted, and the anesthesia box was rotated 90° every 15 s. When the mouse could not turn itself prone onto all four limbs from an abnormal position, this indicated the loss of righting reflex (LORR), which was recorded as the anesthesia induction time and marked the beginning of the anesthesia maintenance phase. The corresponding experimental operation was performed during the maintenance phase according to the experimental design. The sevoflurane volatilization tank was closed at 30 min of anesthesia to stop inhalation anesthesia, and the residual sevoflurane in the anesthesia box and pipeline was removed by rapid oxygenation (the gas composition was 80% oxygen and 20% nitrogen) at a constant flow rate of 2 L/min. The recovery of righting reflex (RORR) was indicated by the mouse being able to voluntarily place all four feet on the floor from an abnormal position. The time between the end of anesthesia and the RORR was recorded as the emergence time. To eliminate the influence of individual mouse differences and experimental environment, the same batch of mice was used for both the control group and the experimental group.

2.3 Stereotaxic localization of mouse brain

After weighing and recording the body weight of the mice, eight-week-old C57BL/6J mice were anesthetized with 1% pentobarbital sodium (50 mg/kg) and fixed the head with a stereotactic apparatus (68018, RWD Life Sciences, Inc., Shenzhen, China); the position of the

skull was adjusted horizontally using an ear bar and nose clip. The eyes of the mice were coated with erythromycin ointment to prevent irreversible damage caused by strong light. Adjust the microscopic field of view and magnification. Using a tissue scissors, carefully trim the hair above the target brain region on the skull surface. Disinfect the area with a 75% alcohol swab from inside to outside. Cut open the cranial skin along the midline and remove the mucosal tissue on the skull surface to fully expose the anterior and posterior fontanelles of the mouse skull. Under a microscope, the injector tip is used for positioning. The tip is lifted and moved to the anterior fontanelle, where the coordinates are set to zero. The tip is then raised to the posterior fontanelle, and the height between the two fontanelles is adjusted to ensure a difference of less than or equal to 0.03 millimeters. After leveling the anterior and posterior fontanelles, equidistant points (2.30 mm) on both sides of the anterior fontanelle are selected to determine the height. If the height difference is within 0.03 millimeters, it is considered that the skull has been leveled. According to the fourth edition of the mouse brain atlas (Paxinos and Franklin, 2013), the target brain region was precisely localized on the skull surface. Once the location was confirmed, a micro handheld cranial drill was carefully used to create a hole with a diameter of 0.5-1 mm. The operation required delicacy, and during drilling, it was crucial to avoid large blood vessels and the cerebral parenchyma to prevent irreversible damage to the brain tissue and ensure the accuracy of experimental results. The body temperature of anesthetized mice was kept constant at 37°C during the procedure using a heating pad. To target the bilateral BLA, the coordinates were AP: -0.40 mm; ML: ±2.95 mm; DV: -5.00 mm. To target the DR, the coordinates were AP: −4.55 mm, ML: −0.44 mm, DV: −2.80 mm, 10° right. Viruses were delivered via a gauge needle for the specification of 10 μL controlled by an Ultra Micro Pump (160494 F10E, WPI). To allow the virus to spread, the syringe was not removed for 10 min after the end of the injection. According to the experimental needs, optical fibers or cannulas were subsequently implanted in the corresponding location and secured with dental cement. After that, the incision was sutured, and the mice were placed on a heating blanket to be transferred to a cage when the mice were awake.

2.4 Implantation of cannula in lateral ventricle and nucleus

After leveling the skull and drilling the target brain region, a small hole (without drilling

through the skull) is drilled on each side of the anterior and posterior fontanelles. Screws are then fixed into these holes, with the criterion being that 1/3 of the screw protrudes from the skull surface and is securely in place. Using a cannula holder to clamp the cannula, maintain the cannula in a vertical position, and slowly insert the cannula into the target brain region. Secure the cannula, screws, and skull tightly with dental cement and powder. Ensure that the skull surface remains dry, as any seepage of blood or tissue fluid may prevent the cannula from being securely fixed and cause it to fall off. After complete solidification, release the cannula holder, insert the cannula core, weigh the mouse again, and record the weight. After the surgery, place the mouse on a constant-temperature electric blanket for recovery. Once the mouse's movements have recovered to normal, return it to its cage. The coordinates of the target brain regions involved in this experiment were CeA (AP−0.37mm, ML±2.80mm, DV −4.95mm) and mPFC (AP+0.90mm, ML±0.45mm, DV−1.50mm). The cannulas used in the experiment were: lateral ventricle cannula (O.D.0.30mm/C.C2.4/M3.5, 62004, RWD Life Science, China) and CeA cannula (O.D.0.50mm/C.C2.4/M3.5, 62004, RWD Life Science, China). In the experiment, the volume of saline or drug injected into the lateral ventricle was 2 μl, and the volume of saline or drug microinjected into the cannula was 200 nl.

2.5 Viral injection into brain nuclei

After skull leveling and drilling of the target brain region under stereotaxic localization, a microinjection pump (RWD Life Science, China) was used to aspirate an appropriate amount of virus. The needle tip was then moved to the position above the corresponding coordinate brain region. After confirming the unobstructed injection, the needle was slowly lowered vertically. During the descent process, careful attention was paid to whether the needle tip deviated to the left or right. After the needle tip reached the target brain region, it was left in place for at least 5 minutes to allow the brain tissue to fully rebound. Then, 100 nl of virus was injected using a microinjection pump at a rate of 20-40 nl/min. After injection, the needle tip remained in the target brain region for at least 10 minutes to prevent virus overflow when withdrawing the needle. After 10 minutes, the needle was withdrawn slowly at a constant speed. During the operation, the skull surface was wetted with a moist sterile cotton ball to prevent skin adhesion, which helps reduce skin tension and facilitate surgical incision suturing. After skin suturing, medical erythromycin ointment was evenly applied to

the incision to prevent wound infection. The mouse was placed on an electric blanket for recovery and returned to its cage after confirming the restoration of spontaneous activity. The next experiment was conducted three weeks after virus infection. The coordinates of the target brain regions involved in this experiment were CeA (AP−0.37mm, ML±2.80mm, DV−4.95mm) and mPFC (AP+0.90mm, ML±0.45mm, DV−1.50mm). The AAV viruses used in the experiment were: pAAV-TPH2 PRO-ChETA-EYFP-WPRES-PAS (100 nl, titer: 10^{13} vg/ml, Shanghai Shengbo Biotechnology), rAAV-TPH2-hM3d(Gq)-EGFP-WPREs (100 nl, titer: 10^{12} vg/ml, Wuhan Shumi), and rAAV-TPH2-hM4D(Gi)-mCherry-WPREs (100 nl, titer: 10^{12} vg/ml, Wuhan Shumi). After 3-4 weeks of virus infection, the next experiment was performed. After the completion of the experiment, the location of virus expression was confirmed through immunohistochemistry.

2.6 Fiber photometry

C57BL/6J mice at 8 weeks of age were anesthetized with 1% pentobarbital sodium (50 mg/kg) and fixed the head with a stereotactic apparatus (68018, RWD Life Sciences, Inc., Shenzhen, China), as previously described. rAAV-TPH2-GCaMP6s-WPRE-hGH-pA virus(100nl, viral titer 1012vg/ml, Brain VTA Technology Co., Ltd., Wuhan, China) was injected into the CeA (AP−0.37mm, ML±2.80mm, DV−4.95mm) and mPFC (AP+0.90mm, ML±0.45mm, DV−1.50mm) based on the mouse brain atlas at a rate of 40 nl/min with a 10-ml microliter syringe controlled by an Ultra Micro Pump (160494 F10E, WPI). The syringe was kept inserted until 10 min after the end of the infusion to allow diffusion of the virus particles. Then, the optical fiber (FOC-W-1.25-200-0.37-4.0, Inper, Hangzhou, China) was im-planted in the CeA (AP−0.37mm, ML±2.80mm, DV−4.95mm) and mPFC (AP+0.90mm, ML±0.45mm, DV−1.50mm). Three weeks after viral injection, optical fibers (FOC-W-1.25–200–0.37–3.0, Inper, Hangzhou, China) were placed 0.05 mm above the virus injection point. Fluorescence emissions were recorded using a fiber photometry system (Inper, Hangzhou, China, C11946) using a 488-nm diode laser, and the mice were placed in a dark box to avoid the influence of natural light source of calcium signal recording and accessed to the computer recording software to record calcium signals. After the recording was completed, the results recorded by the optical fiber were read into the calcium signaling data analysis software. change in fluorescence values ($\Delta F/F$) was calculated as $(F - F0)/F0$.

2.7 Retrograde tracing

C57BL/6J mice at 8 weeks of age were anesthetized with 1% pentobarbital sodium (50 mg/kg) and fixed the head with a stereotactic apparatus (68018, RWD Life Sciences, Inc., Shenzhen, China), as previously described. As for the CTB-555 retrograde tracing from the mPFC to the CeA: 100nl of CTB-555 (1 μg/μl, BrainVTA Technology Co., Ltd., Wuhan, China) was injected in the CeA with a total content of 100 nl for retrograde labeling of projection neurons. The following experiments were performed at least one week after surgery to ensure the expression of virus. As for the RV virus cross-synaptic tracing, the Tph2-dependent helper viral vectors (rAAV-EF1a-DIO-mCherry-F2A-TVA-WPRE-hGE polyA, rAAV-EF1α-DIO-oRVG -WPRE-hGE polyA and rAAV-TPH2-CRE-WPRE-hGE polyA) (100nl, titer 60nl/min, Brain VTA Technology Co., Ltd., Wuhan, China) were injected into the CeA. Three weeks later, RV-EnvA-ΔG-EGFP (100nl, titer 20nl/min, Brain VTA Technology Co., Ltd., Wuhan, China) was injected into the CeA. Seven days later, sacrificed the mice and observed RV-labeled neurons in the mPFC.

2.8 Optogenetics

Three weeks after the injection of optogenetic virus (pAAV-TPH2 PRO-ChETA-EYFP-WPRES-PAS), the fiber optic cannula (FOC-W-1.25-200-0.37-3.0, Yingbo Technology Co., Ltd., Hangzhou, China) was implanted under the stereotaxic apparatus. The fiber optic cannula was clamped at the end of the fiber holder, and the skull of the mouse was leveled using the tip of the fiber, following the same steps as the virus injection. Three shallow holes were drilled on the skull surface away from the target brain region, and screws were implanted for fixing the skull and the cannula. The cannula was positioned 0.05-0.1mm above the target nucleus, and a mixture of dental cement and powder was used to tightly bound the fiber optic cannula, screws, and skull. One week after the implantation of the fiber, optogenetic experiments were performed. Before the experiment, the laser intensity at the end of the laser was measured using an optical power meter, and the laser parameters were adjusted according to the experimental protocol. The laser was connected to the cannula on the mouse's head via a fiber optic patch cord. The specific principle of optogenetics is to utilize a viral vector to introduce a light-sensitive protein gene (the light-sensitive channel protein ChETA, a mutant of ChR2) into specific types of neurons, allowing the expression of

light-sensitive channel proteins in the target brain region. Under excitation light of a specific wavelength (the excitation light for ChETA protein is blue light with a wavelength around 465nm), the light-sensitive protein can be transformed into an ion channel. For example, when ChETA is irradiated with blue light, it transforms into a cation channel, allowing sodium ions to flow inward, leading to neuronal depolarization and subsequently inducing action potentials. In this experiment, blue light was used to activate 5-HT neurons (expressing ChETA) in the CeA and mPFC. The light intensity parameters of the laser were adjusted, and an optical power meter was used to detect the laser intensity reaching the end of the cannula, controlling the laser within the required experimental range.

2.9 Chemogenetics

Three weeks after injecting the chemogenetic viruses rAAV-TPH2-hM3d(Gq)-EGFP-WPRE or rAAV-TPH2-hM4D(Gi)-mCherry-WPREs into the CeA or mPFC, different concentrations of clozapine-N-oxide (CNO) were prepared according to the experimental protocol. CNO was dissolved in saline and injected intraperitoneally 10 minutes before sevoflurane anesthesia to manipulate the target brain regions and observe its effects on behavior. The specific principle of chemogenetics involves using a viral vector to introduce Designer Receptor Exclusively Activated by Designer Drugs (DREADDs) receptors, which are modified from G protein-coupled receptors, into specific types of neurons. By activating or inhibiting the DREADDs receptors with CNO, the corresponding GPCR signaling pathways can be selectively activated. CNO acts on cells expressing hM3Dq to depolarize them, enhancing cell excitability. Conversely, CNO acts on cells expressing hM4Di to hyperpolarize them, inhibiting their excitability.

2.10 Immunohistochemistry

After the experiment, the anesthetized mouse was fixed on a foam board with its limbs. Using the left hand, a hemostatic clamp was used to hold the skin, while the right hand employed a scalpel to cut open the abdominal skin along the abdominal cavity, exposing the mouse's liver and diaphragm. With a pair of tweezers, the xiphoid process was grasped, and the diaphragm was cut open to fully expose the heart. It was crucial to avoid puncturing the heart. A perfusion needle was inserted into the left ventricle of the mouse, and a small incision was made in the right auricle. Phosphate-buffered saline (PBS) was slowly perfused through

the needle until the mouse's liver and extremities turned from red to white. Subsequently, 4% paraformaldehyde (PFA) was continuously perfused until the limbs became rigid, the tail displayed spastic reactions, and the neck stiffened. During the perfusion, care was taken to minimize perfusion into the pulmonary circulation. After the perfusion, the head was cut off using a large scissor. The brain tissue was completely separated from the skull using a tissue scissor and tweezers, and immediately immersed in 4% PFA for fixation in a 4℃ refrigerator. After 24 hours, the brain was removed and placed in a 30% sucrose solution for dehydration (approximately 24 hours). Once the brain tissue was completely immersed in the sucrose solution, 35-40 μm thick coronal brain slices were cut using a cryostat (CM30503, Leica). The brain slices were placed in a well plate containing PBS and washed on a shaker for 3 times, 5 minutes each. They were then incubated in blocking solution at room temperature for 2 hours. After discarding the blocking solution, the primary antibody diluent was added and incubated overnight on a 4℃ shaker. After incubation, the brain slices were washed with PBS to remove non-specific adsorption, with 3 washes of 10 minutes each. Subsequently, the brain slices were placed in the secondary antibody diluent and incubated for 1 hour at room temperature, avoiding light exposure. After incubation, the slices were washed with PBS for 3 times, 15 minutes each. The brain slices were flattened on glass slides, stained with DAPI for 7 minutes for nuclear staining, and excess DAPI was washed away with PBS. Finally, the slides were mounted with anti-fade mounting medium. All images were captured using a Nikon A1R confocal microscope (Nikon, Japan) or a VS120 microscope (Olympus, Japan), and positive cell co-localization was analyzed using ImageJ (NIH, Baltimore). The positions of the virus, optical fiber, and cannula were confirmed for all experimental mice, and only mice with correct positions were used for result analysis.

2.11 Quantification and statistical analysis

The experimental data were reported as mean ± SD. The Shapiro–Wilk normality test was performed for all experimental data before data analysis. For between-group comparisons, normally distributed data were compared using the Student's T-test, including independent samples T-test and paired samples T-test, and non-normally distributed data were compared using the Mann–Whitney U test or Wilcoxon signed-rank test. The Levene test was used to detect the homogeneity of square difference. After the data met the normal distribution and

homogeneity of variance, ordinary one-way ANOVA analysis was used for comparing three or more groups, and two-way ANOVA analysis and Bonferroni's test were used for comparisons between two factors and different groups. Statistical significance was indicated by $P < 0.05$. In this study, GraphPad Prism8.0 and SPSS version 26.0 were used for the statistical analysis of data.

3 Results

3.1 Exogenous supplementation of 5-HTP significantly shortens the recovery time from sevoflurane anesthesia

3.1.1 Intraperitoneal injection of 5-HTP reduced the recovery time of sevoflurane anesthesia in a dose-dependent manner

To investigate the impact of whole-body 5-HT expression on the induction and recovery of sevoflurane anesthesia, we selected wild-type C57BL/6J mice aged 8 weeks as experimental animals. In the experimental group, mice were intraperitoneally injected with different concentrations of 5-HTP, a synthetic precursor of 5-HT. Twenty-four hours after the initial injection, 5-HTP was administered again intraperitoneally. In the control group, mice were injected with saline. One hour later, the mice were placed in an anesthesia chamber for anesthesia induction, and the induction time was recorded. After maintaining anesthesia for 30 minutes, anesthesia was stopped, and the recovery time was recorded (Fig.1A). Firstly, compared with the control group, intraperitoneal injection of different concentrations of 5-HTP had no significant effect on the induction time of sevoflurane anesthesia ($P<0.05$, Fig.1B). When compared with the control group, intraperitoneal injection of 25 mg/kg 5-HTP had no significant impact on the recovery time of sevoflurane anesthesia, while intraperitoneal injection of 50 mg/kg ($P<0.05$) and 75 mg/kg ($P<0.01$) 5-HTP significantly shortened the recovery time of sevoflurane anesthesia (Fig.1C). These results indicate that exogenous supplementation of 5-HTP and elevation of whole-body 5-HT levels can promote anesthesia recovery.

3.1.2 Intracerebroventricular injection of 5-HTP promote recovery from anesthesia

To investigate the effect of brain 5-HT levels on the induction and recovery of sevoflurane anesthesia, lateral ventricular cannulas were implanted into the brains of mice in the control and experimental groups one week before the experiment, and the mice were

allowed to rest for a week after surgery (Fig.1N). Fifteen minutes before the experiment, the control group received an injection of saline through the cannula, while the experimental groups received different concentrations of 5-HTP (Fig.1D). Compared with the control group, an intracerebroventricular injection of 11.35 mol/L 5-HTP did not significantly affect the induction and recovery time of sevoflurane anesthesia (P>0.05, Fig.1E-F). Although intracerebroventricular injection of 22.7 mol/L 5-HTP had no significant effect on the induction time of sevoflurane anesthesia (P >0.05, Fig.1E), it significantly shortened the recovery time compared to the control group (P<0.001, Fig.1F). These results suggest that increasing brain 5-HT levels can promote recovery from anesthesia.

3.1.3 Microinjection of 5-HTP into the CeA shortens the recovery time from sevoflurane anesthesia by activating CeA 5-HT neurons

To further investigate the effect of elevating 5-HT levels in the CeA on the induction and recovery of sevoflurane anesthesia, intracranial cannulas were implanted into the CeA of mice in the control and experimental groups one week before the experiment. After surgery, the mice were allowed a week to recover (Fig.1O). Fifteen minutes before the experiment, the control group received an injection of saline by the cannula, while the experimental group received various concentrations of 5-HTP (Fig.1G). Compared with the control group, intranuclear injection of 2.5 mg/ml and 5 mg/ml 5-HTP did not significantly affect the induction of sevoflurane anesthesia (P>0.05, Fig.1H). However, intranuclear injection of 2.5 mg/ml (P<0.01) and 5 mg/ml (P <0.001) 5-HTP significantly shortened the recovery time from sevoflurane anesthesia (Fig.1I). These data suggest that exogenous supplementation of 5-HTP, which elevates 5-HT levels, can promote recovery from sevoflurane anesthesia by activating CeA 5-HT neurons.

3.2 The pro-arousal effects of increased 5-HT in CeA can be reversed by 5-HT1A receptor antagonist microinjected in mPFC

To investigate the specific targets of CeA serotonergic neurons in regulating the recovery process from sevoflurane anesthesia, we first conducted pharmacological experiments. Cannulas were implanted into the unilateral CeA and mPFC of C57BL/6J mice (Fig.1O-P). Experiments were conducted one week after surgery to allow the mice to recover. Fifteen minutes before sevoflurane anesthesia, saline or 5.0 mg/ml 5-HTP was injected into the CeA

nucleus. The mice were then placed placement in an anesthesia chamber for inhalation of 3.0% sevoflurane for anesthesia induction and maintenance. At the 20th minute of anesthesia maintenance, 5.0 mg/ml, or 10.0 mg/ml WAY-100635 (5-HT1A receptor antagonist) was microinjected into the mPFC nucleus, and changes in the recovery behavior of the mice were observed (Fig.1J). The experimental results showed no significant difference in the induction time of sevoflurane anesthesia among the groups (P>0.05, Fig.1K). Compare with mice received 5.0 mg/ml 5-HTP in the CeA, 5 mg/ml WAY-100635 in mPFC increased the recovery time from sevoflurane anesthesia (P<0.01, Fig.1L). These results indicate that antagonizing 5-HT1A receptors in the mPFC can reverse the positive effect of activating 5-HT neurons in the CeA on promoting recovery, suggesting that 5-HT1A receptors in the mPFC may be specific targets for CeA 5-HT neurons involved in regulating the recovery from sevoflurane anesthesia.

3.3 The activity of CeA and mPFC 5-HT neurons was inhibited during sevoflurane anesthesia which can be reversed by 5-HTP

Given the arousal-promoting effects of CeA-specific exogenous 5-HTP supplementation, we focused our attention on CeA 5-HT neurons. Our immunohistochemical results revealed that the activity of CeA 5-HT neurons decreased after sevoflurane anesthesia, suggesting a crucial role for CeA 5-HT neurons in regulating arousal from sevoflurane anesthesia. As a preliminary step toward identifying the role of CeA, we used fiber photometry to assess the altered activity of CeA 5-HT neurons at different stages of sevoflurane anesthesia (Fig.2A). We injected rAAV-TPH2-GCaMP6S-WPRE-hGH-pA into the CeA of C57BL/6J mice and examined changes in GCaMP6S fluorescence signal through an optical fiber located in the CeA (Fig.2B). Our findings indicated that calcium signaling in CeA 5-HT neurons significantly diminished following LORR and augmented subsequent to RORR. During the sevoflurane anesthesia phase, the ΔF/F peak of calcium signaling in CeA 5-HT neurons was significantly reduced relative to other stages (P<0.05, Fig.2C-E).

We combined pharmacological methods with fiber photometry to investigate the effects of exogenous 5-HTP supplementation on the activity of CeA 5-HT neurons. Following a three-week post-injection period of a calcium signal virus in the CeA, mice received an intraperitoneal injection of 75 mg/kg 5-HTP or saline, with a repeated dose administered 1

hour before sevoflurane anesthesia. The calcium activity of CeA 5-HT neurons at various stages of sevoflurane anesthesia was measured, assessing neuronal activity during the RORR stage (Fig.2F). We found that, compared to the control group, the ΔF/F peak of calcium signaling of CeA 5-HT neurons was significantly elevated during the RORR stage following 5-HTP administration ($P<0.05$, Fig.2G-I), which suggests that the increased activity of CeA 5-HT neurons facilitates arousal from sevoflurane anesthesia.

Given that pharmacological studies have shown that microinjection of antagonists into the mPFC can reverse pro-arousal effects, we further investigated the activity of mPFC 5-HT neurons during sevoflurane anesthesia. The experimental protocol was consistent with the aforementioned procedures (Fig.3A), with virus injections performed three weeks prior to the sevoflurane anesthesia experiment (Fig.3B), the calcium signal in mPFC neurons of mice infected with GCaMP6s in mPFC was recorded by photometry. Compared with the wakefulness, LORR and RORR stages, the calcium signal activity wave of Sevoflurane stages was reduced, and the decrease of the ΔF/F peak of calcium signaling in mPFC 5-HT neurons was particularly significant ($P<0.05$, Fig.3C-E). Further, regarding the arousal-promoting effects of 5-HTP (Fig.3F), intraperitoneal injection of 75mg/kg 5-HTP enhanced the calcium signal activity wave of sevoflurane anesthesia during the RORR stage (Fig.3G), and the ΔF/F peak of calcium signaling of mPFC 5-HT neurons significantly amplified during the RORR stage compared with the control group ($P<0.05$, Fig.3H-I). Combined the results of pharmacology and fiber photometry, it is evident that exogenous supplementation of 5-HTP promotes the recovery-promoting effect of 5-HT neurons in the CeA and mPFC.

3.4 The existence of 5-HTergic projection relationship between the CeA and mPFC

Based on the above experimental data, the CeA and mPFC 5-HT neurons play a crucial role in the sevoflurane anesthesia recovery process. Furthermore, we focused on the projection relationship between the two regions, we took advantage of retrograde tracing techniques that permits direct visualization of the anatomical projections. We initially injected a retrograde tracer cholera toxin subunit B-555 (CTB-555) into the CeA that allowed the CTB to spread retrogradely into the mPFC neurons (Fig.4A-B) and observed that CTB labeled the projecting Tph2(+) neurons in mPFC by immunofluorescence staining (Fig.4C). Furthermore, to assess the functional synaptic connectivity of the CeA and mPFC 5-HT neurons, we constructed RV-

helper retrograde trans-monosynaptic tracing system. The Tph2-dependent helper viruses (rAAV-EF1a-DIO-mCherry-F2A-TVA-WPRE-hGE polyA, rAAV-EF1α-DIO-oRVG -WPRE-hGE polyA and rAAV-TPH2-CRE-WPRE-hGE polyA) were injected into the CeA, which facilitated monosynaptic retrograde RV spread to infect Tph2(+) neurons. Three weeks later, rabies virus (RV-EnvA-ΔG-EGFP) was injected into the CeA. Seven days later, sacrificed the mice and observed RV-labeled neurons in the mPFC (Fig.4D, left). We recognized the RV-helper retrograde trans-monosynaptic tracing system subsequently infected CeA 5-HT neurons that expressed the Tph2-dependent helper (Fig.4D, up). Similar to the findings in CTB-555 retrograde labeling, we visualized a substantial number of Tph2(+) neurons colocalized with RV in the mPFC, which were identified as 5-HT neurons, indicating the presence of 5-HTergic projection between the CeA and mPFC (Fig.4D, down). These data indicate that 5-HTergic neurons in the mPFC provide an input to CeA neurons.

3.5 Optogenetic activation of CeA 5-HT neurons reduced the recovery time from sevoflurane anesthesia

To activate 5-HT neurons more precisely in the CeA, we utilized optogenetics by injecting the ChETA virus pAAV-TPH2 PRO-ChETA-EYFP-WPRES-PAS carrying the specific promoter TPH2 into the unilateral or bilateral CeA of mice (Fig.5J). Three weeks after virus infection, optical fibers were implanted above the CeA (0.05-0.1 mm) to enable 465 nm blue light to reach the target brain region (Fig.5M). During the 20th minute of maintenance under 3% sevoflurane anesthesia, the experimental group received blue light irradiation with different light intensities (5 mW/10 mW/15 mW, all at 20 Hz 20 ms) until the mice regained their righting reflex (Fig.5A, 5L). The control group did not receive light irradiation, and anesthesia induction and recovery times were recorded. The results showed that different lighting parameters had no significant difference in the induction time of sevoflurane anesthesia (P>0.05, Fig.5B). Activation of bilateral CeA with 10 mW (P<0.05) and 15 mW (P<0.01) of light intensity significantly reduced the recovery time from sevoflurane anesthesia (Fig.5C), and the degree of reduction in recovery time was correlated with light intensity, that 15 mW of light significantly shortened the anesthesia recovery time compared to 10 mW.

Subsequently, we compared the differences in the shortening of sevoflurane anesthesia

recovery time by unilateral and bilateral light exposure. At the 20th minute of anesthesia maintenance, 15 mW blue light was used to activate 5-HT neurons in the left, right, and bilateral CeA. Experimental results showed that unilateral or bilateral optogenetic activation of CeA 5-HT neurons significantly shortened the recovery time from sevoflurane anesthesia ($P<0.01$, Fig.5C), and there was no significant difference in the shortening of sevoflurane anesthesia recovery time among the three different light exposure methods targeting the left, right, or bilateral brain regions ($P>0.05$, Fig.5C). Analysis of these data suggests that specific activation of 5-HT neurons in the CeA can significantly shorten the recovery time from sevoflurane anesthesia in mice, and the degree of shortening is related to the degree of 5-HT neuron activation. Furthermore, there was no statistical difference in the effect of unilateral or bilateral light exposure on the CeA. Additionally, the number of c-fos(+)/Tph2(+) cells in the nucleus of the bilateral CeA experimental group exposed to 15 mW blue light was significantly higher than that in the saline group ($P<0.001$, Fig.5K, 5P). These data indicate that optogenetic activation of CeA 5-HT neurons can shorten the recovery time from sevoflurane anesthesia and promote post-anesthesia consciousness recovery.

3.6 Chemogenetic activation of CeA 5-HT neurons promotes arousal from sevoflurane anesthesia

To exclude the potential influence of CNO itself on the anesthesia process, we injected experimental doses of CNO (0.5 mg/kg and 1.0 mg/kg) intraperitoneally into mice that had not been injected with the virus (Fig.S1A). Compared with the control group, intraperitoneal injection of different concentrations of CNO had no significant impact on the induction and recovery time of sevoflurane anesthesia ($P>0.05$, Fig.S1B-C).

Three weeks prior to the experiment, we injected the chemogenetic activation virus rAAV-TPH2-hM3d(Gq)-EGFP-WPRE or the inhibition virus rAAV-TPH2-hM4D(Gi)-mCherry-WPREs carrying a specific TPH2 promoter into the bilateral CeA brain regions of 8-week-old mice (Fig.6D, 6N-O). Behavioral experiments were conducted three weeks after viral infection. Ten minutes before anesthesia, the experimental groups received intraperitoneal injections of 0.25mg/kg or 0.5mg/kg CNO (Fig.6A). Used chemogenetic activation of CeA 5-HT neurons in general anesthesia, we obtained results similar to those of optogenetics. The experimental groups receiving intraperitoneal injections of 0.25mg/kg and

0.5mg/kg CNO showed no significant difference in anesthesia induction time compared to the control group (P>0.05, Fig.6B). Conversely, intraperitoneal injections of 0.25mg/kg (P<0.05) and 0.5mg/kg (P<0.01) CNO to activate bilateral CeA significantly shortened the anesthesia recovery time (Fig.6C). Moreover, the experimental group receiving 0.5mg/kg CNO intraperitoneally showed significantly more c-fos(+)/Tph2(+) cells in the CeA than the saline group (P<0.001, Fig.6E-F). These data indicate that the activation of CeA 5-HT neurons through chemogenetics can shorten the sevoflurane anesthesia recovery time and promote consciousness recovery after general anesthesia.

Furthermore, we attempted to inhibit the activity of CeA 5-HT neurons (Fig.6K). Results indicated that IP injection of 0.25 mg/kg CNO did not significantly alter the recovery time compared to the control group (P>0.05, Fig.6L); Conversely, IP injection of 0.5 mg/kg CNO significantly prolonged the recovery time (P<0.01, Fig.6M). These results further suggest that the bidirectional modulation of recovery time by CeA 5-HT neurons.

3.7 Involvement of 5-HT1A and 5-HT2A/C receptors in CeA-mPFC 5-HTergic neural circuit modulating arousal from sevoflurane anesthesia

To investigate the specific targets of CeA 5-HT neurons in regulating the recovery process from sevoflurane anesthesia, we employed a combination of pharmacological and genetic techniques to manipulate CeA 5-HT neurons more precisely and verify the specific roles of 5-HT1A and 2A/C receptors in the mPFC in regulating sevoflurane anesthesia. Three weeks before the general anesthesia experiment, an optogenetic virus (pAAV-TPH2 PRO-ChETA-EYFP-WPRES-PAS) was injected into the lateral CeA. After three weeks of viral transfection, an optical fiber was implanted approximately 0.1 mm above the CeA, and a cannula was implanted in the mPFC (Fig.5O). Experiments were conducted one week after surgery. The mice were placed in an anesthesia chamber, and at the 20th minute of anesthesia maintenance, 1 mg/ml or 2 mg/ml of 5-HT2A/C receptor antagonist was microinjected into the mPFC nucleus. Immediately after drug administration, blue light stimulation (15 mw, 20 Hz, 20 ms) was applied to the CeA to observe changes in the recovery behavior of the mice (Fig.5D). The experimental results showed that mPFC injection of 1mg/ml (P<0.05) and 2mg/ml (P<0.01) KET significantly reversed the arousal-promoting effect of activating CeA 5-HT neurons (Fig.5F), and this phenomenon was more pronounced in the mPFC injection

group with 2 mg/ml KET (P< 0.01, Fig.5F). The experimental results suggest that 5-HT2A/C receptors in the mPFC may be important targets for CeA 5-HT neurons to regulate the recovery from sevoflurane anesthesia. The role of the 5-HT1A receptor was studied using the aforementioned methods. After three weeks of viral transfection, an optical fiber was implanted approximately 0.1 mm above the CeA, and lateral ventricular cannulas were implanted (Fig.5N). The mice were placed in an anesthesia chamber, and at the 20th minute of anesthesia maintenance, intracerebroventricular injection of 5 mg/ml or 10 mg/ml 5-HT1A receptor antagonist (Fig.5G). The experimental results showed that ICV injection of 10 mg/ml WAY significantly reversed the arousal-promoting effect of activating CeA 5-HT neurons (P<0.01, Fig.5I), and there was no significant impact in the ICV injection group with 5 mg/ml KET (P>0.05, Fig.5I).

Based on the above findings, we combined pharmacological and chemogenetic techniques. Three weeks before the experiment, the chemogenetic virus (rAAV-TPH2-hM3d(Gq)-EGFP-WPRE) was injected into bilateral CeA. After two weeks of viral infection, cannulas were implanted unilaterally in the mPFC (Fig.6G), and behavioral experiments were conducted one week after surgery. Ten minutes before the general anesthesia experiment, 0.5 mg/kg CNO was injected intraperitoneally to activate serotonergic neurons in the CeA (Fig.6H). The results showed no significant difference in the recovery time from sevoflurane anesthesia among the groups compared to the control group (P>0.05, Fig.6I). Conversely, we observed that microinjection of 10 mg/ml WAY-100635 (P<0.05), 2 mg/ml KET (P<0.05), and 4 mg/ml KET(P<0.01) into the mPFC significantly reversed the shortening of recovery time mediated by chemically activated serotonergic neurons in the CeA (Fig.6J). This phenomenon was more pronounced in the group with 4 mg/ml KET microinjected into the mPFC (P<0.01, Fig.6J). These experimental results indicate that both 5-HT1A and 2A/C receptor antagonists can reverse the arousal-promoting effect of activating serotonergic neurons in the CeA, and 5-HT1A and 2A/C receptors may be specific targets for CeA 5-HT neurons to regulate the recovery from sevoflurane anesthesia.

3.8 Activation of the mPFC 5-HT neurons reduced the recovery time from sevoflurane anesthesia

Previous studies have suggested that the central amygdala receives widespread inputs

from both the cerebral cortex and subcortical areas. Therefore, we further investigated the potential role of 5-HT neurons in the mPFC during sevoflurane anesthesia. One week before the experiment, cannulas were implanted unilaterally in the mPFC of 8-week-old mice (Fig.7D). After a week of rest, the mice underwent general anesthesia experiments. Different concentrations of 5-HT were microinjected into the mPFC 15 minutes before the start of anesthesia, and the changes in induction and recovery behaviors of the mice were observed (Fig.7A). The results showed no significant difference in induction time between the control group and the experimental groups ($P>0.05$, Fig.7B). Injection of 2.5 mg/ml 5-HT into the mPFC in the experimental group significantly shortened the recovery time from sevoflurane anesthesia ($P<0.05$, Fig.7C). Additionally, the effects of 5.0 mg/ml and 10.0 mg/ml 5-HT injected into the mPFC on shortening the recovery time from sevoflurane anesthesia were more pronounced ($P<0.01$, Fig.7C). These results indicate that increasing 5-HT levels in the mPFC and activating 5-HT neurons in the mPFC can promote recovery from sevoflurane anesthesia.

To enhance the specificity of activation of mPFC 5-HT neurons, a virus carrying a Tph2-promoter was injected into the unilateral mPFC, and chemogenetic manipulation was performed three weeks after viral infection (Fig.S2H). Ten minutes before the anesthesia experiment, IP injection of saline or 0.25 mg/kg, 0.5 mg/kg, and 1.0 mg/kg CNO was administered to activate 5-HT neurons in the mPFC to varying degrees (Fig.S2B). The experimental results suggested that there was no significant difference in the sevoflurane anesthesia induction time between the experimental groups and the control group ($P>0.05$, Fig.S2E). Experimental groups receiving IP injection of 0.25 mg/kg and 0.5 mg/kg CNO showed no significant difference in the sevoflurane anesthesia recovery time compared to the saline group ($P>0.05$, Fig.S2F). Conversely, IP injection of 1.0 mg/kg CNO significantly shortened the sevoflurane anesthesia recovery time ($P<0.05$, Fig.S2F). Furthermore, the experimental group (IP 1.0 mg/kg CNO) exhibited significantly more c-fos(+)/Tph2(+) cells in the mPFC compared to the saline-injected control group ($P<0.01$, Fig.7K, 7L).

In addition to chemogenetics, we further utilized optogenetics to validate the function of 5-HT neurons in mPFC. Specifically, a virus specifically infecting 5-HT neurons was injected into the lateral mPFC (Fig.S2G). After three weeks of viral infection, an optical fiber was

implanted 0.1 mm above the mPFC region. One-week post-surgery, optogenetic experiments were conducted (Fig.S2A). The results indicated that there were no significant differences in sevoflurane anesthesia induction times across groups (P>0.05, Fig.S2C). In the experimental group, various light parameters were used. Compared to the control group, activation of unilateral mPFC 5-HT neurons at 5mW did not significantly affect recovery times from sevoflurane anesthesia (P>0.05, Fig.S2D). However, increasing the light intensity to 10mW significantly shortened the anesthesia recovery times (P<0.05, Fig.S2D). At a light intensity of 15mW, the pro-arousal effect of activating 5-HT neurons was even more pronounced (P<0.001, Fig.S2D). These data indicate that activating CeA 5-HT neurons through optogenetics and chemogenetics can promote recovery from sevoflurane anesthesia. Our experimental data, obtained through pharmacological, optogenetic, and chemogenetic experiments, suggest that increasing 5-HT levels in the mPFC has a role in promoting recovery from sevoflurane anesthesia. Specifically, 5-HT neurons in the mPFC are involved in regulating recovery from sevoflurane anesthesia, and specifically activating 5-HT neurons has the effect of shortening anesthesia recovery time.

3.9 The pro-arousal effects of chemogenetic or optogenetics activation of mPFC 5-HT neurons can be reversed by 5-HT1A and 5-HT2A/C receptor antagonist microinjected in CeA

Previous studies have indicated the close projection between the mPFC and CeA, prompting us to further explore whether 5-HT neurons in the mPFC exert regulatory effects by acting on 5-HT1A or 2A/C receptors in the CeA. Firstly, we conducted a combined optogenetics and pharmacology experiment. In C57BL/6J mice, a virus specifically infecting 5-HT-producing neurons was injected into the unilateral mPFC (Fig.7P-Q). Three weeks after infection, an optical fiber was implanted 0.1 mm above the mPFC, and a cannula was implanted into the lateral CeA. After one week of recovery, optogenetic experiments were performed. At the 20th minute of anesthesia maintenance, 5mg/ml WAY-100635 or 1mg/ml KET was microinjected into the CeA nucleus. Immediately after the microinjection, 15mW blue light was used to stimulate the mPFC, and changes in mouse behavior were observed (Fig.7M). Compared to the control group, there was no significant difference in the sevoflurane anesthesia induction time between the light-stimulated group and the antagonist +

light-stimulated group (P>0.05, Fig.7N). Injection of 5 mg/ml WAY-100635 into the CeA to antagonize the 5-HT 1A receptor significantly reversed the recovery-promoting effect exerted by activating 5-HT neurons in the mPFC (P<0.01, Fig.7O). Similarly, injection of 1mg/ml KET into the CeA to antagonize the 5-HT 2A/C receptor also reversed the recovery-promoting effect of activating 5-HT neurons in the mPFC (P<0.001, Fig.7O). Compared to mice without optogenetics activation in mPFC, the optogenetics enhanced the number of c-fos(+)/Tph2(+) cells in the nucleus of the mPFC (Fig.7R)

To validate this result, we combined chemogenetics and pharmacology techniques. A chemogenetic activation virus was injected into the unilateral mPFC (Fig.7I-J). And a cannula was implanted into the unilateral CeA two weeks after infection (Fig.7H). Chemical genetic experiments were performed after one week of recovery. Ten minutes before the start of anesthesia, 1.0 mg/kg CNO was injected intraperitoneally to specifically activate 5-HT neurons in the mPFC. At the 20th minute of anesthesia maintenance, 2mg/ml and 4mg/ml KET were microinjected into the CeA nucleus (Fig.7E). There was no significant difference in the sevoflurane anesthesia induction time between the experimental and control groups (P>0.05, Fig.7F). Observation of the mice's anesthesia recovery time revealed that intra-CeA injection of 2mg/ml KET to antagonize 5-HT2A/C receptors significantly prolonged the sevoflurane anesthesia recovery time in the experimental group (P<0.01, Fig.7G). This phenomenon was more pronounced in the experimental group with 4mg/ml KET injection into the CeA (P<0.001, Fig.7G).

These experimental results indicate that both 5-HT1A and 2A/C receptor antagonists can reverse the positive arousal-promoting effect of activating 5-HT neurons in the CeA, suggesting that 5-HT1A and 2A/C receptors may be the specific targets of 5-HT-producing neurons in the CeA that regulate sevoflurane anesthesia recovery.

4 Discussion

Sevoflurane, a common inhalational anesthetic, holds significant value in surgical and diagnostic procedures. Despite increasing clinical and fundamental research into the effects of sevoflurane on behavior and consciousness, the central mechanisms by which it alters consciousness are complex, leaving the specific neural mechanisms unclear. The specific

mechanisms behind reversible loss of consciousness during general anesthesia continue to be a focal point in anesthesiology research. Owing to shared characteristics between anesthesia and natural sleep, mechanisms involving the endogenous sleep-wake system and neural network modulation of anesthesia-related consciousness changes have become a research hotspot in recent years.

5-HT, a crucial monoamine neurotransmitter, plays a significant role in the functions related to consciousness within the central nervous system, with ample experimental evidence supporting its critical involvement in sleep-wake regulation[32]. Given the complexity of its receptor system[33], 5-HT interacts through seven distinct receptor types, each subdivided into several subtypes. Consequently, numerous experiments have yielded contradictory results[34], thus far precluding a definitive classification of 5-HT as either a sleep-promoting or wakefulness-promoting agent. Our recent series of studies indicate that activating DR 5-HT neurons and its projections to the BLA can effectively reduce the recovery time from sevoflurane anesthesia. Importantly, different 5-HT autoreceptors may play significant roles in facilitating anesthesia arousal, particularly as both presynaptic 5-HT1A autoreceptors in the DR and postsynaptic 5-HT1A receptors in the BLA exhibit similar arousal-promoting effects[15,35]. Therefore, in this study, we aim to further investigate the 5-HTergic neural circuits associated with consciousness alterations under sevoflurane anesthesia, building upon previous findings.

The activation of the brain relies on numerous regions capable of concurrently receiving diverse signals, among which the ascending reticular activating system (ARAS) is pivotal in initiating and sustaining wakefulness[36]. CeA is a crucial component of the ARAS, playing a significant role in maintaining wakefulness and vigilance[37]. Previous studies suggest close projections between mPFC and CeA, with the mPFC exhibiting a widespread distribution of 5-HT receptors. Current research indicates that inhibition of mPFC neurons can delay arousal from general anesthesia in rats, underscoring the critical role of mPFC in regulating consciousness state and arousal process[38]. Further research has revealed that during general anesthesia, 5-HT expression in the mPFC diminish[39]. Consequently, we further focus on the impact of the CeA-mPFC 5-HTergic neural circuit and its receptors, examining their role in the mechanisms underlying consciousness transitions during general anesthesia.

Initially, we conducted pharmacological experiments to verify that exogenously elevating 5-HT can facilitate arousal from 3% sevoflurane anesthesia. We observed that enhancing 5-HT within the brain, and specifically in the CeA significantly shortened the sevoflurane anesthesia recovery time. Concurrently, microinjections of the 5-HT1A receptor antagonist WAY-100635 within the mPFC reversed the arousal-promoting effect. Subsequently, our focus shifted to CeA 5-HT neurons, which activity diminished following sevoflurane anesthesia. We further explored the effects of activating CeA 5-HT neurons on post-anesthetic arousal. Given that optogenetics and chemogenetics allow for continuous and reversible manipulation in neuroscience research, we integrated these precise and targeted techniques with behavioral measurement to conduct our experiments. Utilizing optogenetics and chemogenetics, we specifically activated CeA 5-HT neurons, consistent with pharmacologically induced arousal from sevoflurane anesthesia. Conversely, chemogenetic inhibition of these neurons prolonged the recovery time.

To investigate the presence of projections between CeA and mPFC, we microinjected the 5-HT1A and 2A/C receptor antagonists, WAY-100635 and KET, into the mPFC prior to activation using optogenetics and chemogenetics. We found that the arousal effect induced by activating CeA 5-HT neurons was reversed by 5-HT1A and 2A/C receptor antagonists. Further, we discovered that specifically optogenetic and chemogenetic activation of mPFC 5-HT neurons significantly reduced the recovery time from sevoflurane anesthesia. Compared to optogenetic activation of CeA 5-HT neurons, the light intensity required to shorten anesthesia recovery times by activation of mPFC 5-HT neurons was higher than that needed for activating CeA 5-HT neurons. A similar phenomenon was observed in chemogenetic activation, where the concentration of CNO injected intraperitoneally to activate mPFC 5-HT neurons was higher than that required to activate CeA 5-HT neurons. This observation indicates variations in the distribution density and activity of 5-HT neurons across different nuclei. To further explore the potential bidirectional projections between CeA and mPFC, we activated mPFC 5-HT neurons and concurrently microinjected 5-HT1A and 2A/C receptor antagonists within the CeA. We found that microinjections of WAY-100635 and KET within the CeA significantly reversed the effect of shortened anesthesia recovery times following activation of mPFC 5-HT neurons. Existing research indicates that 5-HT can stimulate

GABAergic neurons by binding to the 5-HT2A/C receptors, thus generating inhibitory postsynaptic currents and serving a role in local negative feedback[40]. Combined with our experimental findings, this further suggests that the 5-HTergic system may exert distinct roles during anesthesia recovery through various receptors. Integrating our optogenetic and chemogenetic activation of 5-HT neurons with exogenous 5-HT supplementation, we postulate that the 5-HT1A and 2A/C receptors play pivotal roles in facilitating recovery from general anesthesia.

Our study elucidates the neural circuits and physiological functions between the CeA and mPFC from behavioral and in vivo neurophysiological perspectives. DRN is a significant source of 5-HT neurons, which project extensively across the brain, including to the CeA[41]. Building on our preliminary findings[15,35], which illustrate the involvement of the DR-BLA 5-HTergic neural circuit in regulating recovery from sevoflurane anesthesia, we hypothesize that the CeA and mPFC may represent secondary and tertiary projection nuclei in this 5-HTergic circuit. The upstream DRN is speculated to regulate this extensive 5-HTergic projection circuit, collectively modulating arousal from sevoflurane anesthesia. Further in-depth investigation is required to elucidate these relationships.

However, the recovery from sevoflurane anesthesia is regulated not solely by this 5-HTergic neural circuit, but also by the concerted actions of multiple brain regions. Current research suggests that due to the extensive distribution of the central 5-HTergic system in the brain, 5-HT cannot be simply classified as promoting wakefulness or sleep; its specific effects on sleep-wake regulation depend on the activation degree and timing of the central 5-HTergic system[42–44]. Sleep onset is induced by 5-HT via the inhibition of cholinergic fibers in the basal forebrain through 5-HT1A receptors[45,46]. With advances in electrophysiology, and neuropharmacology, significant progress has been made in experiments concerning the role of 5-HT in sleep-wake regulation. However, given the widespread distribution of 5-HT neurons across various nuclei and the considerable variability in 5-HT receptor distribution among brain regions[12], the role of 5-HT in regulating general anesthesia arousal warrants further investigation.

There are also some limitations in our study. Firstly, the central nervous circuits involved in arousal from general anesthesia may intersect with other sleep-wake regulatory neural

circuits. Previous studies have shown that the CeA and the locus coeruleus are anatomically interconnected, participating in the regulation of the sleep-wake cycle[47–49]. The cholinergic ascending arousal system, GABAergic sleep-promoting system, dopaminergic system, orexinergic system, and noradrenergic system may interact with the 5-HTergic circuits. They function in the arousal from sevoflurane anesthesia through neurotransmitter release and receptor interaction on various neurons, forming neural circuits. Further research is needed to differentiate between these systems and investigate their mechanisms in sleep-wake regulation. Secondly, as part of the ARAS, the CeA and mPFC not only project to each other but also are widely connected with many other arousal-promoting nuclei. Hence, they may simultaneously receive neural projections and neurotransmitters from other brain regions. In the future, we will conduct in-depth research on the neural activity between the CeA-mPFC and other brain regions during arousal from general anesthesia. Moreover, studies have found that other 5-HT receptors, such as 5-HT3 and 5-HT6 receptors, also play roles in promoting arousal[50,51]. The roles of these receptors in arousal from general anesthesia require further investigation. Therefore, more in-depth, and comprehensive research is urgently needed to determine the underlying neural mechanisms of consciousness transitions related to general anesthesia.

In summary, our research, utilizing pharmacology, fiber photometry, optogenetics, and chemogenetics, provides compelling evidence that the activation of CeA-mPFC 5-HTergic neural circuits is sufficient to facilitate the restoration of consciousness during sevoflurane anesthesia. 5-HT1A and 2A/C mediate the regulation of this recovery process, aiding in the improvement of delayed consciousness recovery due to excessively deep sevoflurane anesthesia. The findings offer new insights into the intricate neural circuit mechanisms underlying the transitions of consciousness during general anesthesia and present effective intervention strategies for addressing delayed recovery of consciousness following sevoflurane anesthesia.

Authors' contributions

H.H.Z. contributed to the conceptualization and design of the study. Y.L.W., Y.Y., Y.X.W. and X.X.X. performed the experiments, analyzed most of the experiments and wrote the draft of the manuscript. Q.X., Z.W.Z. and X.Y.D. helped with the analysis of the experiments and

participated in the modification. All authors contributed to the final version of the manuscript.

Acknowledgments

We thank YuDong Zhou and Yi Shen for their help in experimental design.

Funding

The work was supported by the National Natural Science Foundation of China (Grant no.: 81771403 and 81974205), the Natural Science Foundation of Zhejiang Province (LZ20H090001), and the Program of New Century 131 outstanding young talent plan top-level of Hang Zhou to HHZ; and by the Natural Science Foundation of Zhejiang Province (LHZY24H090003) to YS.

Data Availability

The data supporting the findings of this study are available within the article. Data will be made available upon reasonable request.

Declarations

Ethics Approval

All procedures were in accordance with the National Institutes of Health Guidelines for the Care and Use of Laboratory Animals and were approved by the Animal Advisory Committee of Zhejiang University.

Consent to Participate

Not applicable.

Consent for Publication

Not applicable.

Competing Interests

The authors declare no competing interests.

5 References

[1] Avidan, M.S., Whitlock, E.L., and Mashour, G.A. (2022). General Anesthesia and Postoperative Neurocognitive Outcomes. JAMA *327*, 36–38. https://doi.org/10.1001/jama.2021.22465.

[2] Yi, T., Wang, N., Huang, J., Wang, Y., Ren, S., Hu, Y., Xia, J., Liao, Y., Li, X., Luo, F., et al. (2023). A Sleep-Specific Midbrain Target for Sevoflurane Anesthesia. Adv. Sci. Weinh. Baden-Wurtt. Ger. *10*, e2300189. https://doi.org/10.1002/advs.202300189.

[3] Dean, J.G., Fields, C.W., Brito, M.A., Silverstein, B.H., Rybicki-Kler, C., Fryzel, A.M.,

Groenhout, T., Liu, T., Mashour, G.A., and Pal, D. (2022). Inactivation of Prefrontal Cortex Attenuates Behavioral Arousal Induced by Stimulation of Basal Forebrain During Sevoflurane Anesthesia. Anesth. Analg. *134*, 1140–1152. https://doi.org/10.1213/ANE.0000000000006011.

[4] Liu, D., Li, J., Wu, J., Dai, J., Chen, X., Huang, Y., Zhang, S., Tian, B., and Mei, W. (2020). Monochromatic Blue Light Activates Suprachiasmatic Nucleus Neuronal Activity and Promotes Arousal in Mice Under Sevoflurane Anesthesia. Front. Neural Circuits *14*, 55. https://doi.org/10.3389/fncir.2020.00055.

[5] Duan, W.-Y., Peng, K., Qin, H.-M., Li, B.-M., Xu, Y.-X., Wang, D.-J., Yu, L., Wang, H., Hu, J., and Wang, Q.-X. (2024). Esketamine accelerates emergence from isoflurane general anaesthesia by activating the paraventricular thalamus glutamatergic neurones in mice. Br. J. Anaesth. *132*, 334–342. https://doi.org/10.1016/j.bja.2023.10.038.

[6] Brown, E.N., Purdon, P.L., and Van Dort, C.J. (2011). General anesthesia and altered states of arousal: a systems neuroscience analysis. Annu. Rev. Neurosci. *34*, 601–628. https://doi.org/10.1146/annurev-neuro-060909-153200.

[7] Moody, O.A., Zhang, E.R., Vincent, K.F., Kato, R., Melonakos, E.D., Nehs, C.J., and Solt, K. (2021). The Neural Circuits Underlying General Anesthesia and Sleep. Anesth. Analg. *132*, 1254–1264. https://doi.org/10.1213/ANE.0000000000005361.

[8] Mashour, G.A., Palanca, B.J., Basner, M., Li, D., Wang, W., Blain-Moraes, S., Lin, N., Maier, K., Muench, M., Tarnal, V., et al. (2021). Recovery of consciousness and cognition after general anesthesia in humans. eLife *10*, e59525. https://doi.org/10.7554/eLife.59525.

[9] Xie, H., Chung, D.Y., Kura, S., Sugimoto, K., Aykan, S.A., Wu, Y., Sakadžić, S., Yaseen, M.A., Boas, D.A., and Ayata, C. (2020). Differential effects of anesthetics on resting state functional connectivity in the mouse. J. Cereb. Blood Flow Metab. Off. J. Int. Soc. Cereb. Blood Flow Metab. *40*, 875–884. https://doi.org/10.1177/0271678X19847123.

[10] Tzabazis, A., Miller, C., Dobrow, M.F., Zheng, K., and Brock-Utne, J.G. (2015). Delayed emergence after anesthesia. J. Clin. Anesth. *27*, 353–360. https://doi.org/10.1016/j.jclinane.2015.03.023.

[11] Trombetta, C., Deogaonkar, A., Deogaonkar, M., Ebrahim, Z., Rezai, A., Machado, A., and Farag, E. (2010). Delayed awakening in dystonia patients undergoing deep brain stimulation surgery. J. Clin. Neurosci. Off. J. Neurosurg. Soc. Australas. *17*, 865–868. https://doi.org/10.1016/j.jocn.2009.11.026.

[12] Okaty, B.W., Commons, K.G., and Dymecki, S.M. (2019). Embracing diversity in the 5-HT neuronal system. Nat. Rev. Neurosci. *20*, 397–424. https://doi.org/10.1038/s41583-019-0151-3.

[13] Iwasaki, K., Komiya, H., Kakizaki, M., Miyoshi, C., Abe, M., Sakimura, K., Funato, H., and Yanagisawa, M. (2018). Ablation of Central Serotonergic Neurons Decreased REM

Sleep and Attenuated Arousal Response. Front. Neurosci. *12*, 535. https://doi.org/10.3389/fnins.2018.00535.

[14] Zhai, X., Yuan, Y., Xu, L., Jiang, J., Li, Y., Yan, Y., and Zhang, L. (2023). Cerebrospinal fluid contacting nucleus and its 5-HT: A new insight into the regulation mechanism of general intravenous anesthesia. Brain Res. *1798*, 148168. https://doi.org/10.1016/j.brainres.2022.148168.

[15] Ma, H., Gu, L., Wang, Y., Xu, Q., Zhang, Y., Shao, W., Yu, Q., Lian, X., Liu, L., Gu, J., et al. (2023). The States of Different 5-HT Receptors Located in the Dorsal Raphe Nucleus Are Crucial for Regulating the Awakening During General Anesthesia. Mol. Neurobiol. *60*, 6931–6948. https://doi.org/10.1007/s12035-023-03519-0.

[16] Moriya, R., Kanamaru, M., Okuma, N., Yoshikawa, A., Tanaka, K.F., Hokari, S., Ohshima, Y., Yamanaka, A., Honma, M., Onimaru, H., et al. (2021). Optogenetic activation of DRN 5-HT neurons induced active wakefulness, not quiet wakefulness. Brain Res. Bull. *177*, 129–142. https://doi.org/10.1016/j.brainresbull.2021.09.019.

[17] Herrera-Solis, A., Herrera-Morales, W., Nunez-Jaramillo, L., and Arias-Carrion, O. (2017). Dopaminergic Modulation of Sleep-Wake States. CNS Neurol. Disord. Drug Targets *16*, 380–386. https://doi.org/10.2174/1871527316666170320145429.

[18] Davis, M. (1992). The role of the amygdala in fear and anxiety. Annu. Rev. Neurosci. *15*, 353–375. https://doi.org/10.1146/annurev.ne.15.030192.002033.

[19] Comoli, E., Ribeiro-Barbosa, E.R., and Canteras, N.S. (2000). Afferent connections of the dorsal premammillary nucleus. J. Comp. Neurol. *423*, 83–98. https://doi.org/10.1002/1096-9861(20000717)423:1<83::aid-cne7>3.0.co;2-3.

[20] Monti, J.M. (2010). The structure of the dorsal raphe nucleus and its relevance to the regulation of sleep and wakefulness. Sleep Med. Rev. *14*, 307–317. https://doi.org/10.1016/j.smrv.2009.11.004.

[21] Calvo, J.M., Badillo, S., Morales-Ramirez, M., and Palacios-Salas, P. (1987). The role of the temporal lobe amygdala in ponto-geniculo-occipital activity and sleep organization in cats. Brain Res. *403*, 22–30. https://doi.org/10.1016/0006-8993(87)90118-1.

[22] Morrison, A.R., Sanford, L.D., and Ross, R.J. (2000). The amygdala: a critical modulator of sensory influence on sleep. Biol. Signals Recept. *9*, 283–296. https://doi.org/10.1159/000014652.

[23] Burlet, S., Leger, L., and Cespuglio, R. (1999). Nitric oxide and sleep in the rat: a puzzling relationship. Neuroscience *92*, 627–639. https://doi.org/10.1016/s0306-4522(99)00031-7.

[24] Ressler, K.J., and Nemeroff, C.B. (2000). Role of serotonergic and noradrenergic systems in the pathophysiology of depression and anxiety disorders. Depress. Anxiety *12 Suppl 1*, 2–19. https://doi.org/10.1002/1520-6394(2000)12:1+<2::AID-DA2>3.0.CO;2-4.

[25] Mao, R., Cavelli, M.L., Findlay, G., Driessen, K., Peterson, M.J., Marshall, W., Tononi,

G., and Cirelli, C. (2024). Behavioral and cortical arousal from sleep, muscimol-induced coma, and anesthesia by direct optogenetic stimulation of cortical neurons. iScience *27*, 109919. https://doi.org/10.1016/j.isci.2024.109919.

[26] Li, Q., Zhang, B., Cao, H., Liu, W., Guo, F., Shen, F., Ye, B., Liu, H., Li, Y., and Liu, Z. (2020). Oxytocin Exerts Antidepressant-like effect by potentiating dopaminergic synaptic transmission in the mPFC. Neuropharmacology *162*, 107836. https://doi.org/10.1016/j.neuropharm.2019.107836.

[27] Xia, C., Zhao, Z., Yu, L., and Yan, M. (2021). The role of the central histaminergic system in emergence from propofol anesthesia in rats model. Ann. Palliat. Med. *10*, 6067–6078. https://doi.org/10.21037/apm-20-2594.

[28] Shoob, S., Buchbinder, N., Shinikamin, O., Gold, O., Baeloha, H., Langberg, T., Zarhin, D., Shapira, I., Braun, G., Habib, N., et al. (2023). Deep brain stimulation of thalamic nucleus reuniens promotes neuronal and cognitive resilience in an Alzheimer's disease mouse model. Nat. Commun. *14*, 7002. https://doi.org/10.1038/s41467-023-42721-5.

[29] Mashour, G.A., Pal, D., and Brown, E.N. (2022). Prefrontal cortex as a key node in arousal circuitry. Trends Neurosci. *45*, 722–732. https://doi.org/10.1016/j.tins.2022.07.002.

[30] Athanason, A.C., Nadav, T., Cates-Gatto, C., Roberts, A.J., Roberto, M., and Varodayan, F.P. (2023). Chronic ethanol alters adrenergic receptor gene expression and produces cognitive deficits in male mice. Neurobiol. Stress *24*, 100542. https://doi.org/10.1016/j.ynstr.2023.100542.

[31] Gao, J., Wu, R., Davis, C., and Li, M. (2018). Activation of 5-HT2A receptor disrupts rat maternal behavior. Neuropharmacology *128*, 96–105. https://doi.org/10.1016/j.neuropharm.2017.09.037.

[32] Maffei, M.E. (2020). 5-Hydroxytryptophan (5-HTP): Natural Occurrence, Analysis, Biosynthesis, Biotechnology, Physiology and Toxicology. Int. J. Mol. Sci. *22*, 181. https://doi.org/10.3390/ijms22010181.

[33] Varnäs, K., Halldin, C., and Hall, H. (2004). Autoradiographic distribution of serotonin transporters and receptor subtypes in human brain. Hum. Brain Mapp. *22*, 246–260. https://doi.org/10.1002/hbm.20035.

[34] Yamada, J., Sugimoto, Y., Wakita, H., and Horisaka, K. (1988). The involvement of serotonergic and dopaminergic systems in hypothermia induced in mice by intracerebroventricular injection of serotonin. Jpn. J. Pharmacol. *48*, 145–148. https://doi.org/10.1254/jjp.48.145.

[35] Yu, Q., Wang, Y., Gu, L., Shao, W., Gu, J., Liu, L., Lian, X., Xu, Q., Zhang, Y., Yang, Y., et al. (2024). Dorsal raphe nucleus to basolateral amygdala 5-HTergic neural circuit modulates restoration of consciousness during sevoflurane anesthesia. Biomed. Pharmacother. Biomedecine Pharmacother. *176*, 116937. https://doi.org/10.1016/j.biopha.2024.116937.

[36] Saper, C.B., Scammell, T.E., and Lu, J. (2005). Hypothalamic regulation of sleep and circadian rhythms. Nature *437*, 1257–1263. https://doi.org/10.1038/nature04284.

[37] Scammell, T.E., Arrigoni, E., and Lipton, J.O. (2017). Neural Circuitry of Wakefulness and Sleep. Neuron *93*, 747–765. https://doi.org/10.1016/j.neuron.2017.01.014.

[38] Mashour, G.A., Pal, D., and Brown, E.N. (2022). Prefrontal cortex as a key node in arousal circuitry. Trends Neurosci. *45*, 722–732. https://doi.org/10.1016/j.tins.2022.07.002.

[39] de Filippo, R., Rost, B.R., Stumpf, A., Cooper, C., Tukker, J.J., Harms, C., Beed, P., and Schmitz, D. (2021). Somatostatin interneurons activated by 5-HT2A receptor suppress slow oscillations in medial entorhinal cortex. eLife *10*, e66960. https://doi.org/10.7554/eLife.66960.

[40] Mukaida, K., Shichino, T., Koyanagi, S., Himukashi, S., and Fukuda, K. (2007). Activity of the serotonergic system during isoflurane anesthesia. Anesth. Analg. *104*, 836–839. https://doi.org/10.1213/01.ane.0000255200.42574.22.

[41] Huang, K.W., Ochandarena, N.E., Philson, A.C., Hyun, M., Birnbaum, J.E., Cicconet, M., and Sabatini, B.L. (2019). Molecular and anatomical organization of the dorsal raphe nucleus. eLife *8*, e46464. https://doi.org/10.7554/eLife.46464.

[42] Morrow, J.D., Vikraman, S., Imeri, L., and Opp, M.R. (2008). Effects of serotonergic activation by 5-hydroxytryptophan on sleep and body temperature of C57BL/6J and interleukin-6-deficient mice are dose and time related. Sleep *31*, 21–33. https://doi.org/10.1093/sleep/31.1.21.

[43] Linthorst, A.C., Flachskamm, C., Hopkins, S.J., Hoadley, M.E., Labeur, M.S., Holsboer, F., and Reul, J.M. (1997). Long-term intracerebroventricular infusion of corticotropin-releasing hormone alters neuroendocrine, neurochemical, autonomic, behavioral, and cytokine responses to a systemic inflammatory challenge. J. Neurosci. Off. J. Soc. Neurosci. *17*, 4448–4460. https://doi.org/10.1523/JNEUROSCI.17-11-04448.1997.

[44] Imeri, L., Mancia, M., Bianchi, S., and Opp, M.R. (2000). 5-Hydroxytryptophan, but not L-tryptophan, alters sleep and brain temperature in rats. Neuroscience *95*, 445–452. https://doi.org/10.1016/s0306-4522(99)00435-2.

[45] Monti, J.M. (2011). Serotonin control of sleep-wake behavior. Sleep Med. Rev. *15*, 269–281. https://doi.org/10.1016/j.smrv.2010.11.003.

[46] Levita, L., Hammack, S.E., Mania, I., Li, X.-Y., Davis, M., and Rainnie, D.G. (2004). 5-hydroxytryptamine1A-like receptor activation in the bed nucleus of the stria terminalis: electrophysiological and behavioral studies. Neuroscience *128*, 583–596. https://doi.org/10.1016/j.neuroscience.2004.06.037.

[47] Aston-Jones, G., and Bloom, F.E. (1981). Activity of norepinephrine-containing locus coeruleus neurons in behaving rats anticipates fluctuations in the sleep-waking cycle. J. Neurosci. Off. J. Soc. Neurosci. *1*, 876–886. https://doi.org/10.1523/JNEUROSCI.01-08-00876.1981.

[48] Park, S.P. (2002). In vivo microdialysis measures of extracellular norepinephrine in the rat amygdala during sleep-wakefulness. J. Korean Med. Sci. *17*, 395–399. https://doi.org/10.3346/jkms.2002.17.3.395.

[49] Shouse, M.N., Staba, R.J., Saquib, S.F., and Farber, P.R. (2000). Monoamines and sleep: microdialysis findings in pons and amygdala. Brain Res. *860*, 181–189. https://doi.org/10.1016/s0006-8993(00)02013-8.

[50] Ponzoni, A., Monti, J.M., and Jantos, H. (1993). The effects of selective activation of the 5-HT3 receptor with m-chlorophenylbiguanide on sleep and wakefulness in the rat. Eur. J. Pharmacol. *249*, 259–264. https://doi.org/10.1016/0014-2999(93)90520-r.

[51] Monti, J.M., and Jantos, H. (2011). Effects of the 5-HT_6 receptor antagonists SB-399885 and RO-4368554 and of the 5-HT(2A) receptor antagonist EMD 281014 on sleep and wakefulness in the rat during both phases of the light-dark cycle. Behav. Brain Res. *216*, 381–388. https://doi.org/10.1016/j.bbr.2010.08.020.

6 Figure legends

Figure 1

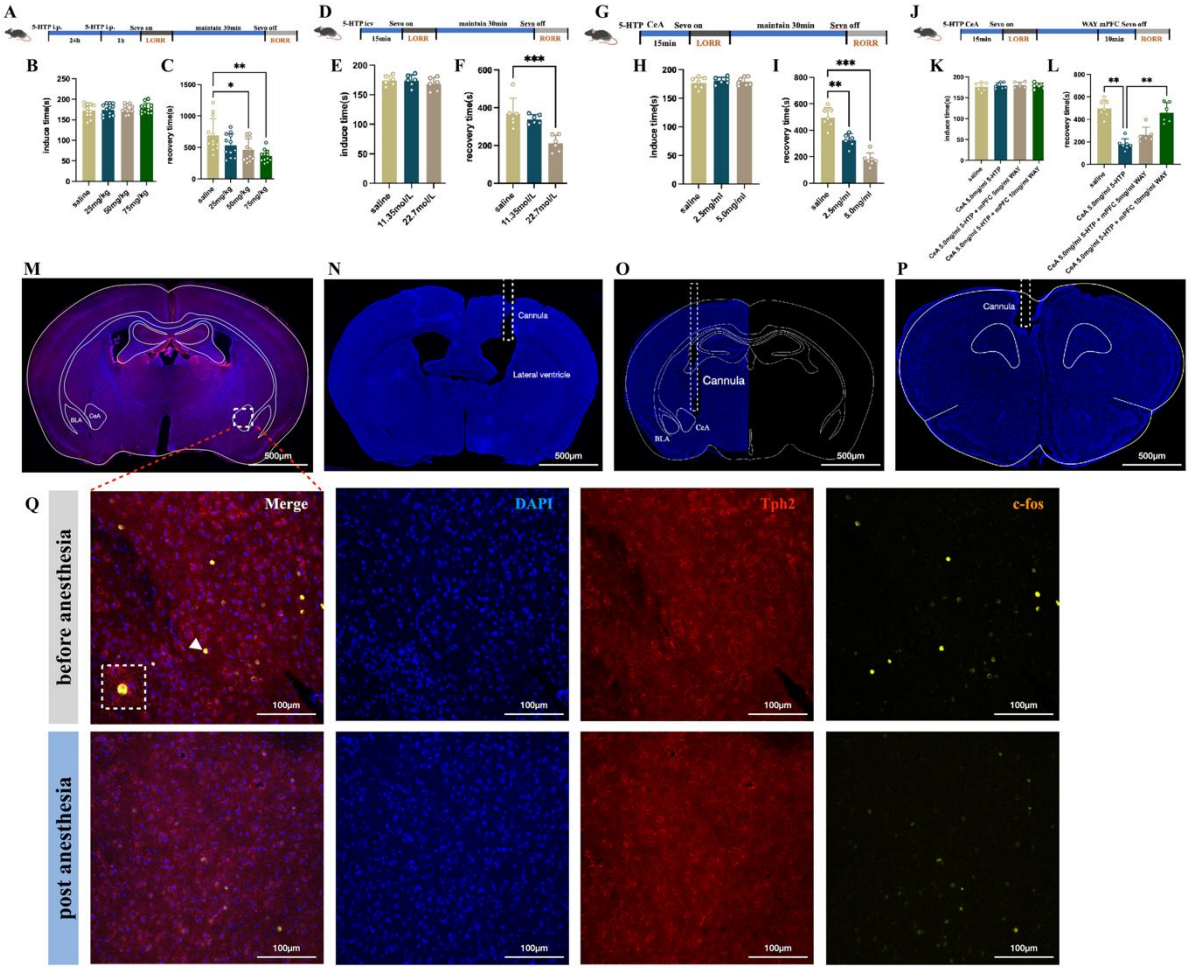

Figure 1. Exogenous supplementation of 5-HTP significantly promotes arousal from sevoflurane anesthesia

(A) Experimental protocol for IP injection of different doses of 5-HTP.

(B, C) Induce time and recovery time for IP injection in saline control, 25 mg/kg 5-HTP, 50 mg/kg 5-HTP, and 75 mg/kg 5-HTP groups.

(D) Experimental protocol for ICV injection of different doses of 5-HTP.

(E, F) Induce time and recovery time for ICV injection in saline control, 11.35 mol/L 5-HTP, and 22.70 mol/L 5-HTP groups.

(G) Experimental protocol for intra-CeA microinjection of 5-HTP.

(H, I) Induce time and recovery time for intra-CeA microinjection in saline control, 2.5 mg/ml 5-HTP, and 5.0 mg/ml 5-HTP groups.

(J) Experimental protocol for intra-CeA microinjection of 5-HTP and intra-mPFC microinjection of 5-HT1A receptor antagonists WAY into lateral mPFC.

(K, L) Induce time and recovery time for the saline control, CeA 5.0 mg/ml 5-HTP, CeA 5.0

mg/ml 5-HTP + mPFC 5mg/ml WAY and CeA 5.0 mg/ml 5-HTP + mPFC 10mg/ml WAY groups.

(M) Representative coronal brain slice of CeA, showing the staining for c-fos, TPH2 and DAPI before anesthesia.

(N) Representative image of the tracks of cannulas implanted into the lateral ICV.

(O) Representative image of the tracks of cannulas implanted into the lateral CeA.

(P) Representative image of the tracks of cannulas implanted into the lateral mPFC.

(Q) Representative images of staining for c-fos, Tph2, and DAPI in the CeA before or after anesthesia.

***$p<0.001$; **$p<0.01$; *$p<0.05$; Data are mean ± SEM; IP, Intraperitoneal injection; ICV, Intracerebroventricular injection; Sevo, Sevoflurane; LORR, Loss of Righting Reflex; RORR, Recovery of Righting Reflex

1 **Figure 2**

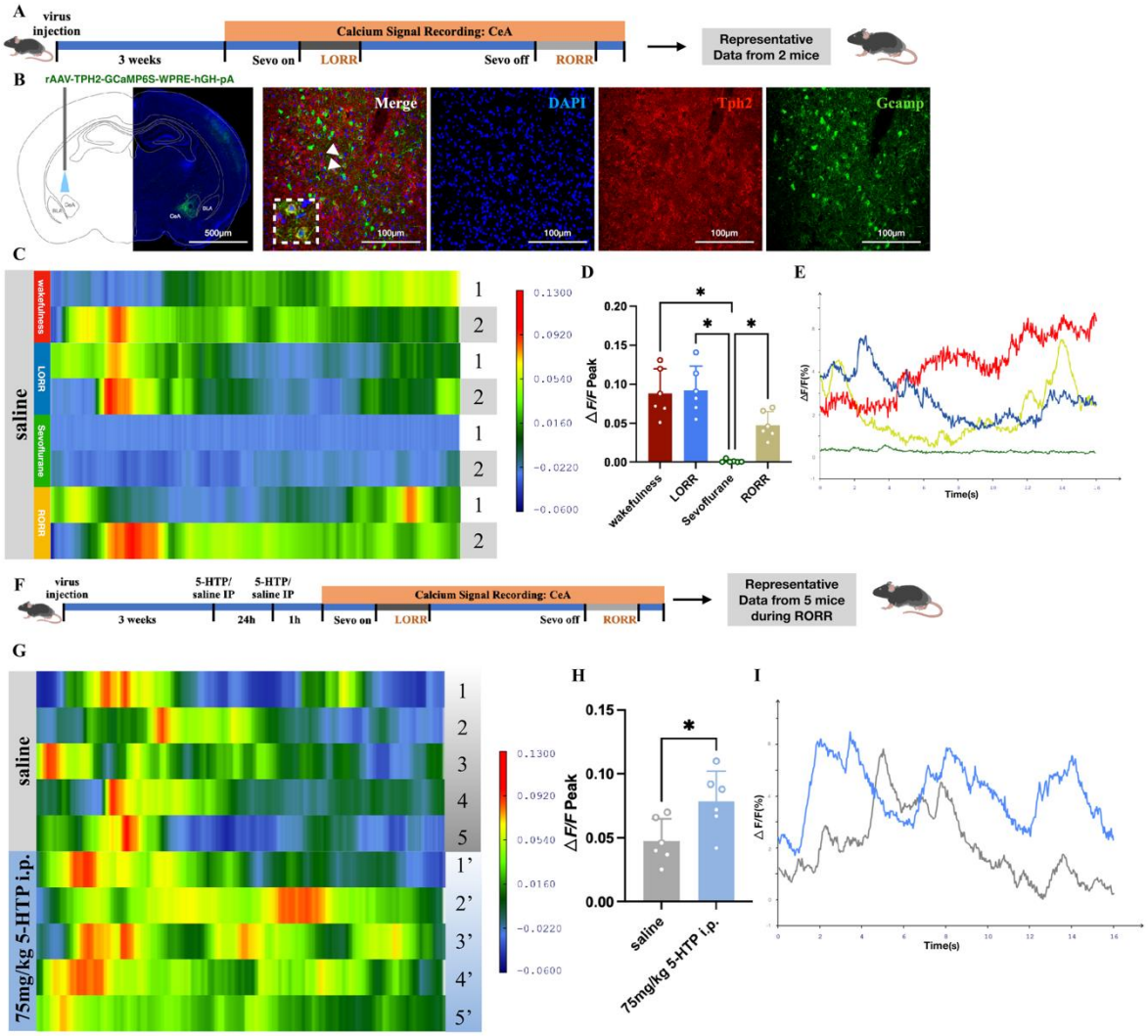

2 **Figure 2. Calcium signaling records recovery time for sevoflurane anesthesia in CeA 5-**
3 **HT neurons and demonstrates the arousal promotion effect of exogenous 5-HTP**
4 **supplementation on sevoflurane anesthesia**

5 **(A)** Experimental protocol for calcium signal recording of CeA 5-HT neurons.

6 **(B)** Representative coronal brain slice, showing the location of virus (rAAV-TPH2-
7 GCaMP6S-WPRE-hGH-pA) injected in the bilateral CeA, and representative images of
8 staining for DAPI, Tph2 and Gcamp in the CeA.

9 **(C-E)** Heatmap and statistical diagram show the activity wave of calcium signals and the
10 peak ΔF/F in the CeA during the wakefulness, LORR, Sevoflurane and RORR four stages.

11 **(F)** Experimental protocol for calcium signal recording of CeA 5-HT neurons and IP
12 injection saline in control and 75mg/kg 5-HTP groups during the RORR stage.

13 **(G-I)** Heatmap and statistical diagram show the activity wave of calcium signals and the peak
14 ΔF/F for IP injection saline in control and 75mg/kg 5-HTP groups in the CeA during the
15 RORR stage.

1 *$p<0.05$; Data are mean ± SEM; IP, Intraperitoneal injection; Sevo, Sevoflurane; LORR, Loss
2 of Righting Reflex; RORR, Recovery of Righting Reflex
3

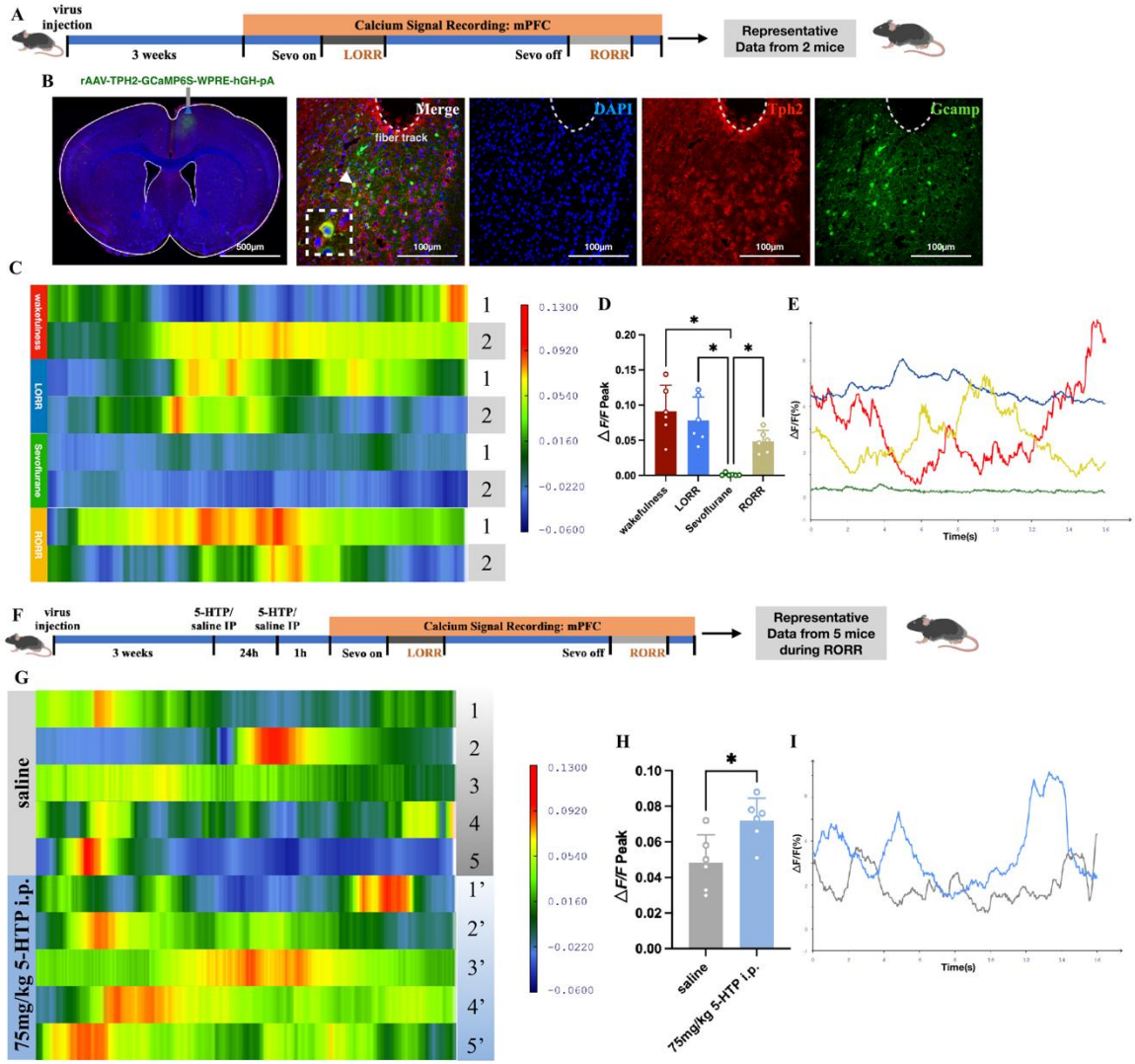

Figure 3

Figure 3. Calcium signaling records recovery time for sevoflurane anesthesia in mPFC 5-HT neurons and demonstrates the arousal promotion effect of exogenous 5-HTP supplementation on sevoflurane anesthesia

(A) Experimental protocol for calcium signal recording of mPFC 5-HT neurons.

(B) Representative coronal brain slice, showing the location of virus (rAAV-TPH2-GCaMP6S-WPRE-hGH-pA) injected in the bilateral mPFC, and representative images of staining for DAPI, Tph2 and Gcamp in the mPFC.

(C-E) Heatmap and statistical diagram show the activity wave of calcium signals and the peak ΔF/F in the mPFC during the wakefulness, LORR, Sevoflurane and RORR four stages.

(F) Experimental protocol for calcium signal recording of mPFC 5-HT neurons and IP injection saline in control and 75mg/kg 5-HTP groups during the RORR stage.

(G-I) Heatmap and statistical diagram show the activity wave of calcium signals and the peak

ΔF/F for IP injection saline in control and 75mg/kg 5-HTP groups in the mPFC during the RORR stage.

*$p<0.05$; Data are mean ± SEM; IP, Intraperitoneal injection; Sevo, Sevoflurane; LORR, Loss of Righting Reflex; RORR, Recovery of Righting Reflex

1 **Figure 4**

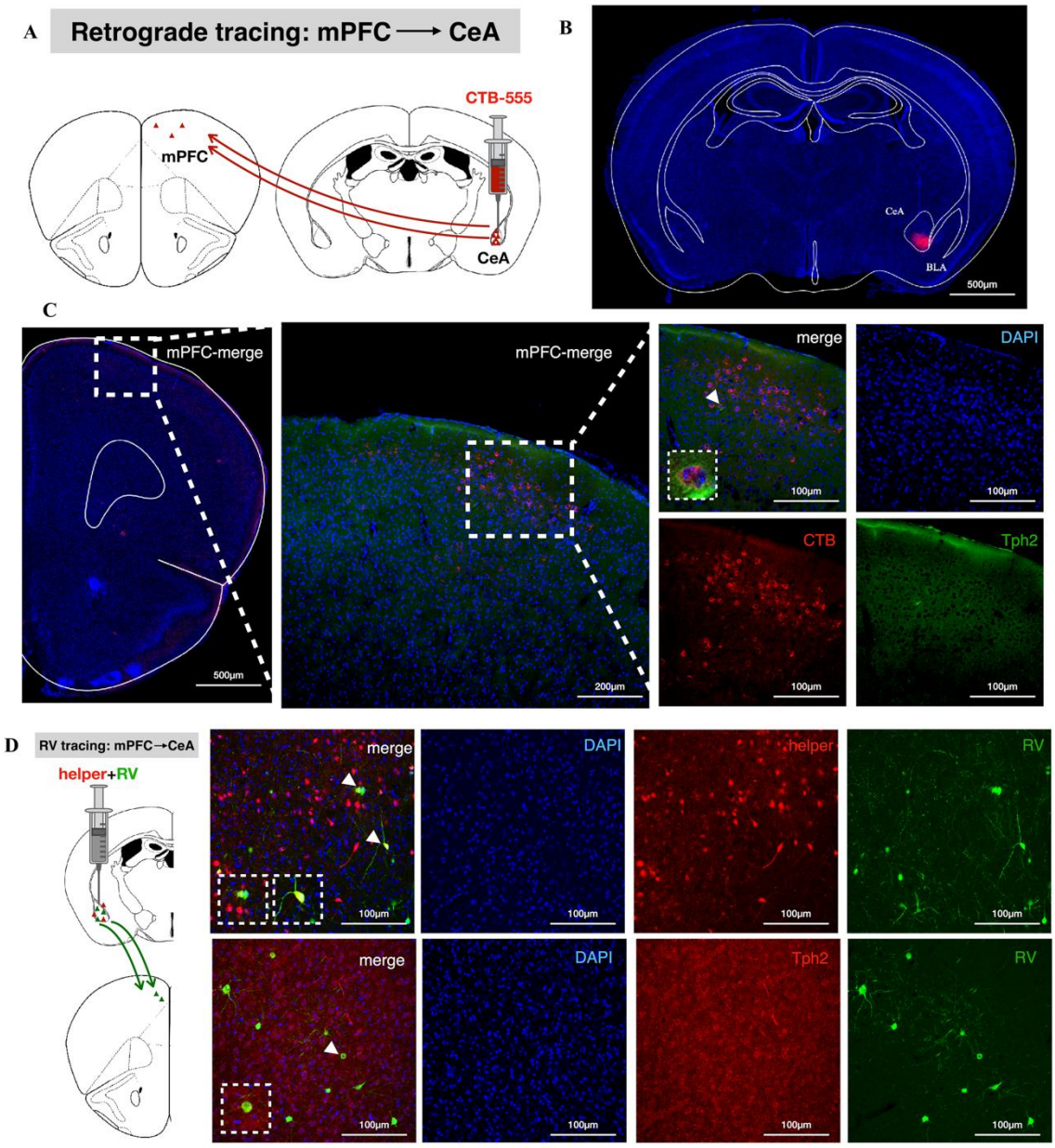

2 **Figure 4. The existence of 5-HTergic projection relationship between the CeA and mPFC**

3 **(A)** Schematic of the position of the virus injection and retrograde labeling.

4 **(B)** Representative coronal brain slice of retrograde labeling.

5 **(C)** Representative images show the co-expression of and staining for CTB and Tph2 in the

6 mPFC.

7 **(D)** Schematic of the position of the virus injection and the retrograde trans-monosynaptic RV

8 tracing. Representative images show the co-expression of and staining for RV and helper in

9 the CeA, and for RV and Tph2 in the mPFC.

10 CTB: Cholera Toxin Subunit B; RV: Rabies Virus

Figure 5

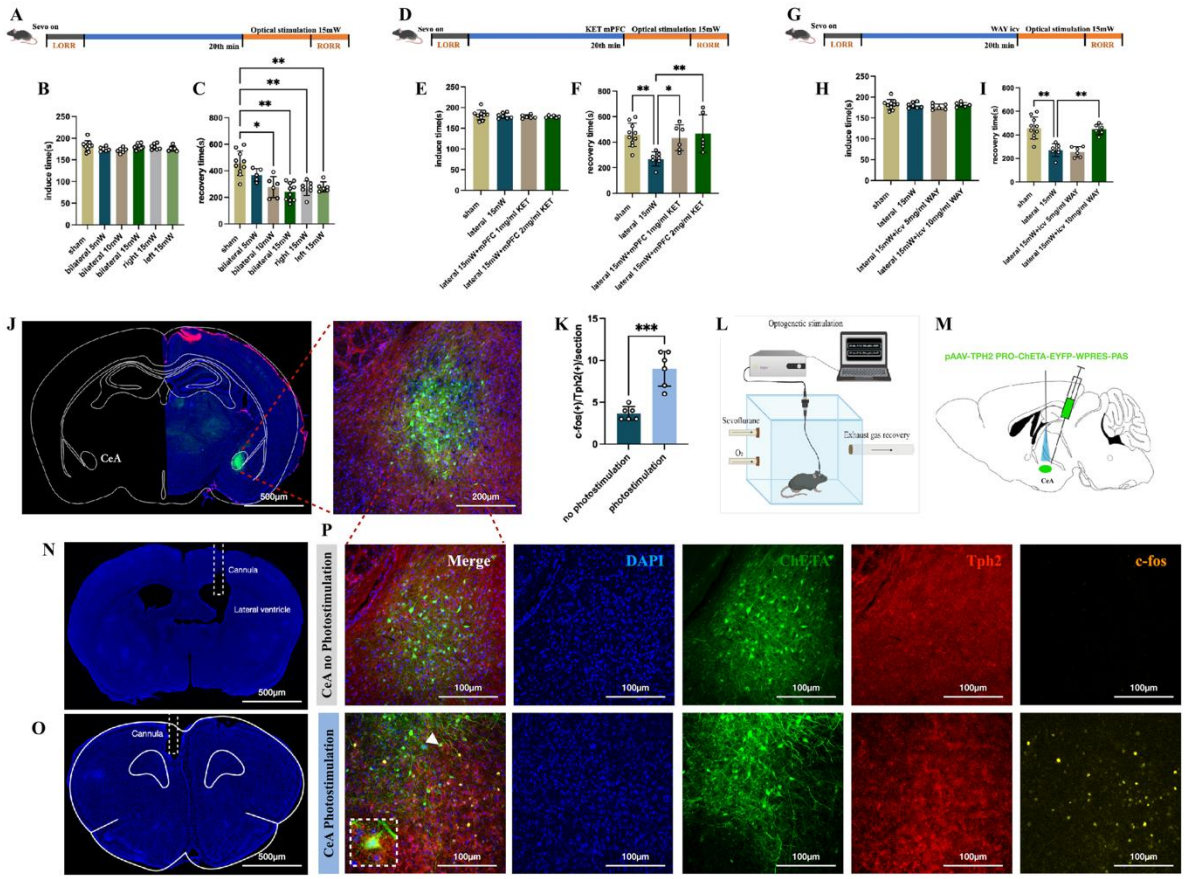

Figure 5. Optogenetic activation of CeA 5-HT neurons reduced the recovery time of sevoflurane anesthesia, and 5-HT1A and 5-HT2A/C receptor antagonist microinjected in mPFC can reverse the effects

(A) Experimental protocol for optogenetic stimulation of CeA 5-HT neurons.

(B, C) Induce time and recovery time for the sham, bilateral 5mW, bilateral 10mW, bilateral 15mW, right 15mW and left 15mW groups.

(D) Experimental protocol for optogenetic activation of CeA 5-HT neurons and microinjection of 5-HT2A/C receptor antagonists KET into lateral mPFC.

(E, F) Induce time and recovery time for the sham, lateral CeA 15mW, lateral CeA 15mW + mPFC 1mg/ml KET and lateral CeA 15mW + mPFC 2mg/ml KET groups.

(G) Experimental protocol for optogenetic activation of CeA 5-HT neurons and microinjection of 5-HT1 receptor antagonists WAY into lateral ICV.

(H, I) Induce time and recovery time for the sham, lateral CeA 15mW, lateral CeA 15mW + ICV 5mg/ml WAY and lateral CeA 15mW + ICV 10mg/ml WAY groups.

(J) Representative coronal brain slice, showing the location of virus (pAAV-TPH2 PRO-ChETA-EYFP-WPRES-PAS) injected in the bilateral CeA.

(K) The quantification of c-fos(+)/Tph2(+) section in the CeA with or without CeA

photostimulation.

(L) A schematic of the optogenetic stimulation device.

(M) Schematic of the position of the virus injection and optic fibers implantation in lateral CeA.

(N) Representative image of the tracks of cannulas implanted into the lateral ICV.

(O) Representative image of the tracks of cannulas implanted into the lateral mPFC.

(P) Representative images of staining for c-fos, Tph2, ChETA and DAPI in the CeA with and without CeA photostimulation.

***$p<0.001$; **$p<0.01$; *$p<0.05$; Data are mean ± SEM; ICV, Intracerebroventricular injection; Sevo, Sevoflurane; LORR, Loss of Righting Reflex; RORR, Recovery of Righting Reflex

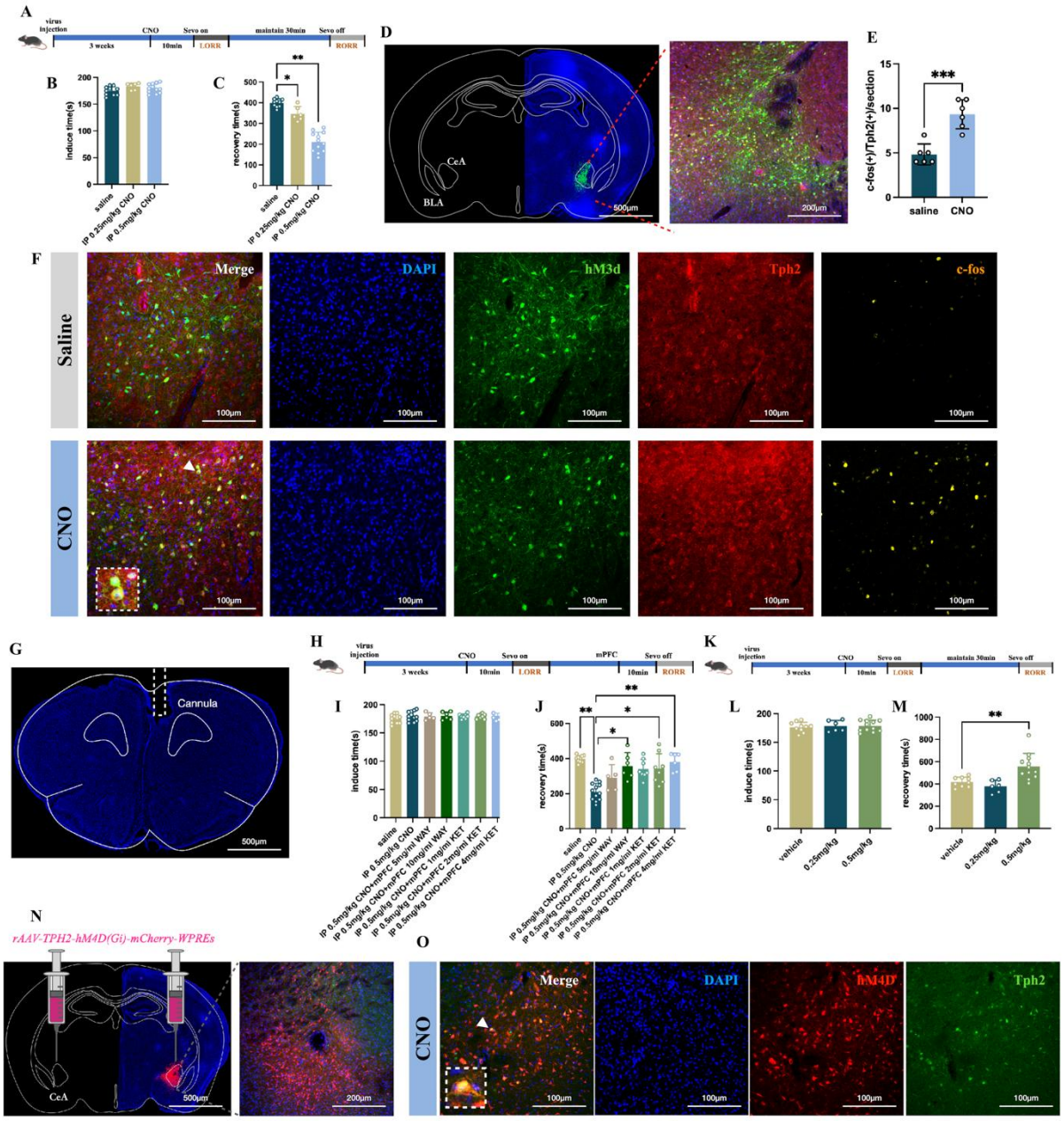

Figure 6

Figure 6. The pro-arousal effects of chemogenetic activation of CeA 5-HT neurons can be reversed by 5-HT1A and 5-HT2A/C receptor antagonist microinjected in mPFC

(A) Experimental protocol for chemogenetic activation of CeA 5-HT neurons. EGFP-WPRE) injected in the bilateral CeA.

(B, C) Recovery time and induce time for IP injection in saline control, 0.25 mg/kg CNO, 0.50 mg/kg CNO groups.

(D) Representative coronal brain slice, showing the location of virus (rAAV-TPH2-hM3D(Gq)- **(E)** The quantification of c-fos(+)/Tph2(+) section in the CeA with or without CNO activation.

(F) Representative images show the co-expression of and staining for c-fos, hM3d, Tph2 and DAPI in the CeA with or without CNO activation.

(G) Representative image of the tracks of cannulas implanted into the lateral mPFC.

(H) Experimental protocol for chemogenetic activation of CeA 5-HT neurons and microinjection of 5-HT1A receptor antagonists WAY or 5-HT2A/C receptor antagonists KET into lateral mPFC.

(I, J) Induce time and recovery time for the sham, IP 0.5 mg/kg CNO, IP 0.5 mg/kg CNO + mPFC 5mg/ml WAY, IP 0.5 mg/kg CNO + mPFC 10mg/ml WAY, IP 0.5 mg/kg CNO + mPFC 1mg/ml KET, IP 0.5 mg/kg CNO + mPFC 2mg/ml KET and IP 0.5 mg/kg CNO + mPFC 4mg/ml KET groups.

(K) Experimental protocol for chemogenetic inhibition of CeA 5-HT neurons.

(L, M) Induce time and recovery time for IP injection in saline control, 0.25 mg/kg CNO, 0.50 mg/kg CNO groups.

(N) Representative coronal brain slice, showing the location of virus (rAAV-TPH2-hM4D(Gi)-mCherry-WPREs) injected in the bilateral CeA.

(O) Representative images show the co-expression of and staining for hM4d, Tph2 and DAPI in the CeA with CNO activation.

***$p<0.001$, **$p<0.01$, *$p<0.05$, Data are mean ± SEM; IP, Intraperitoneal injection; Sevo, Sevoflurane; LORR, Loss of Righting Reflex; RORR, Recovery of Righting Reflex

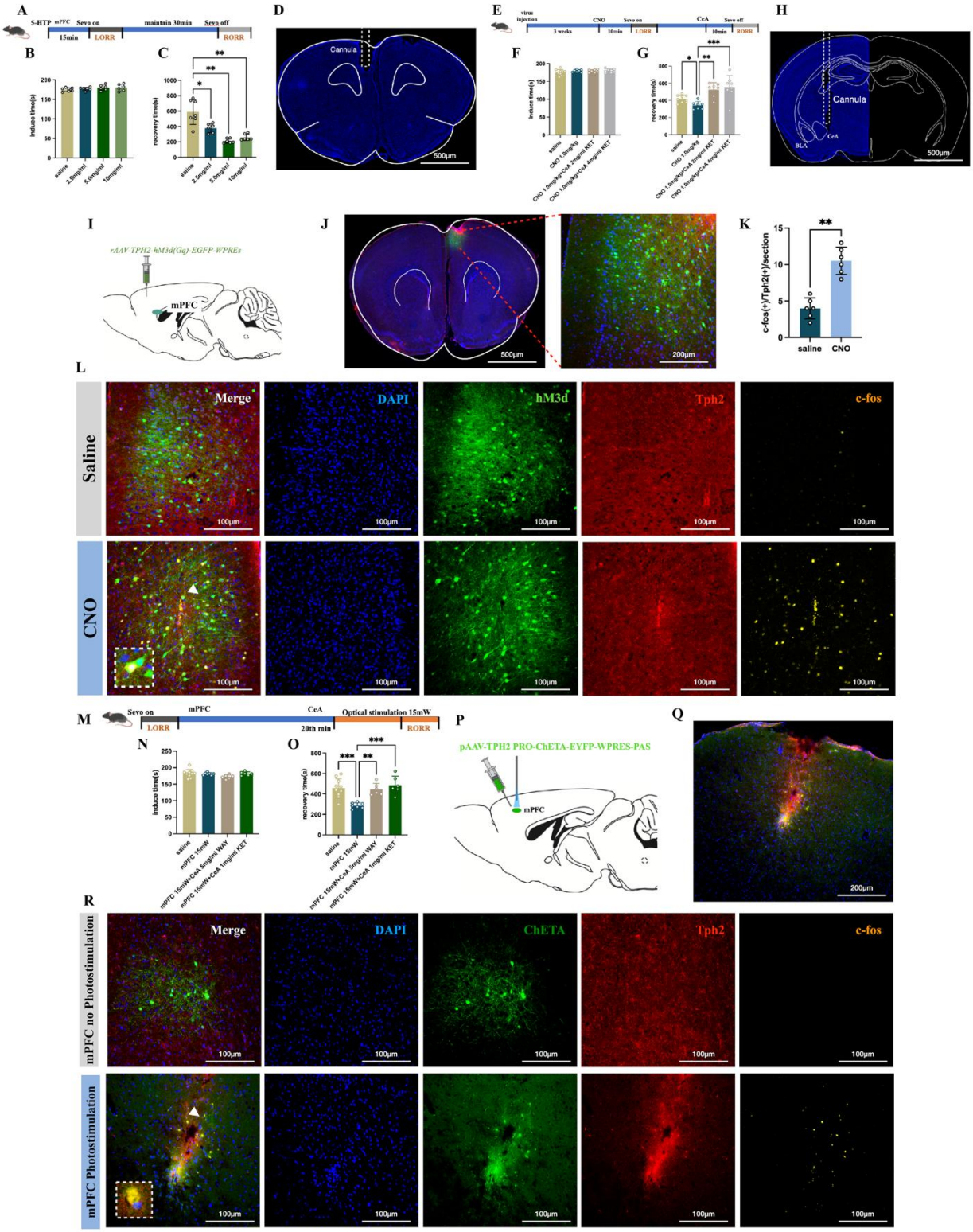

Figure 7

Figure 7. Optogenetic and chemogenetic activation of mPFC 5-HT neurons combined with 5-HT1A and 5-HT2A/C receptor antagonist microinjected in CeA reveals the existence of 5-HTergic bidirectional projection relationship between the CeA and mPFC

(A) Experimental protocol for intra-mPFC microinjection of 5-HTP.

(B, C) Induce time and recovery time for intra-mPFC microinjection in saline control, 2.5 mg/ml 5-HTP, 5.0 mg/ml 5-HTP and 10 mg/ml 5-HTP groups.

(D) Representative image of the tracks of cannulas implanted into the lateral mPFC.

(E) Experimental protocol for chemogenetic activation of mPFC 5-HT neurons and microinjection of 5-HT1A receptor antagonists WAY or 5-HT2A/C receptor antagonists KET into lateral CeA.

(F, G) Induce time and recovery time for the saline control, IP 1.0 mg/kg CNO, IP 1.0 mg/kg CNO + CeA 2mg/ml KET and IP 1.0 mg/kg CNO + CeA 4mg/ml KET groups.

(H) Representative image of the tracks of cannulas implanted into the lateral CeA.

(I) Schematic of the position of the virus injection in lateral mPFC.

(J) Representative coronal brain slice, showing the location of virus (rAAV-TPH2-hM3D(Gq)-EGFP-WPRE) injected in the lateral mPFC.

(K) The quantification of c-fos(+)/Tph2(+) section in the mPFC with or without CNO activation.

(L) Representative images show the co-expression of and staining for c-fos, hM3d, Tph2 and DAPI in the mPFC with or without CNO activation.

(M) Experimental protocol for optogenetic activation of mPFC 5-HT neurons and microinjection of 5-HT1A receptor antagonists WAY or 5-HT2A/C receptor antagonists KET into lateral CeA.

(N, O) Induce time and recovery time for intra-mPFC microinjection in saline control, 2.5 mg/ml 5-HTP, 5.0 mg/ml 5-HTP and 10 mg/ml 5-HTP groups.

(P) Schematic of the position of the virus injection in lateral mPFC.

(Q) Representative coronal brain slice, showing the location of virus (pAAV-TPH2 PRO-ChETA-EYFP-WPRES-PAS) injected in the lateral mPFC.

(R) Representative images of staining for c-fos, Tph2, ChETA and DAPI in the mPFC with and without mPFC photostimulation.

***$p<0.001$, **$p<0.01$, *$p<0.05$, Data are mean ± SEM; Sevo, Sevoflurane; LORR, Loss of Righting Reflex; RORR, Recovery of Righting Reflex

7 Supplementary materials

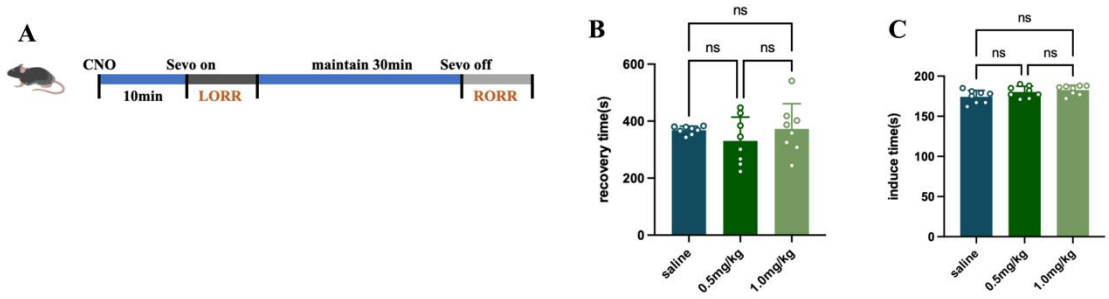

Figure S1

Figure S1. No effect of IP injection of CNO alone on induce time and recovery time of sevoflurane anesthesia

(A) Experimental protocol for IP injection of different doses of CNO.

(B) Recovery time for IP injection in saline control, 0.5 mg/kg CNO and 1.0 mg/kg CNO groups.

(C) Induce time for IP injection in saline control, 0.5 mg/kg CNO and 1.0 mg/kg CNO groups.

ns, $p>0.05$; IP, Intraperitoneal injection; Sevo, sevoflurane; LORR, Loss of Righting Reflex; RORR, Recovery of Righting Reflex

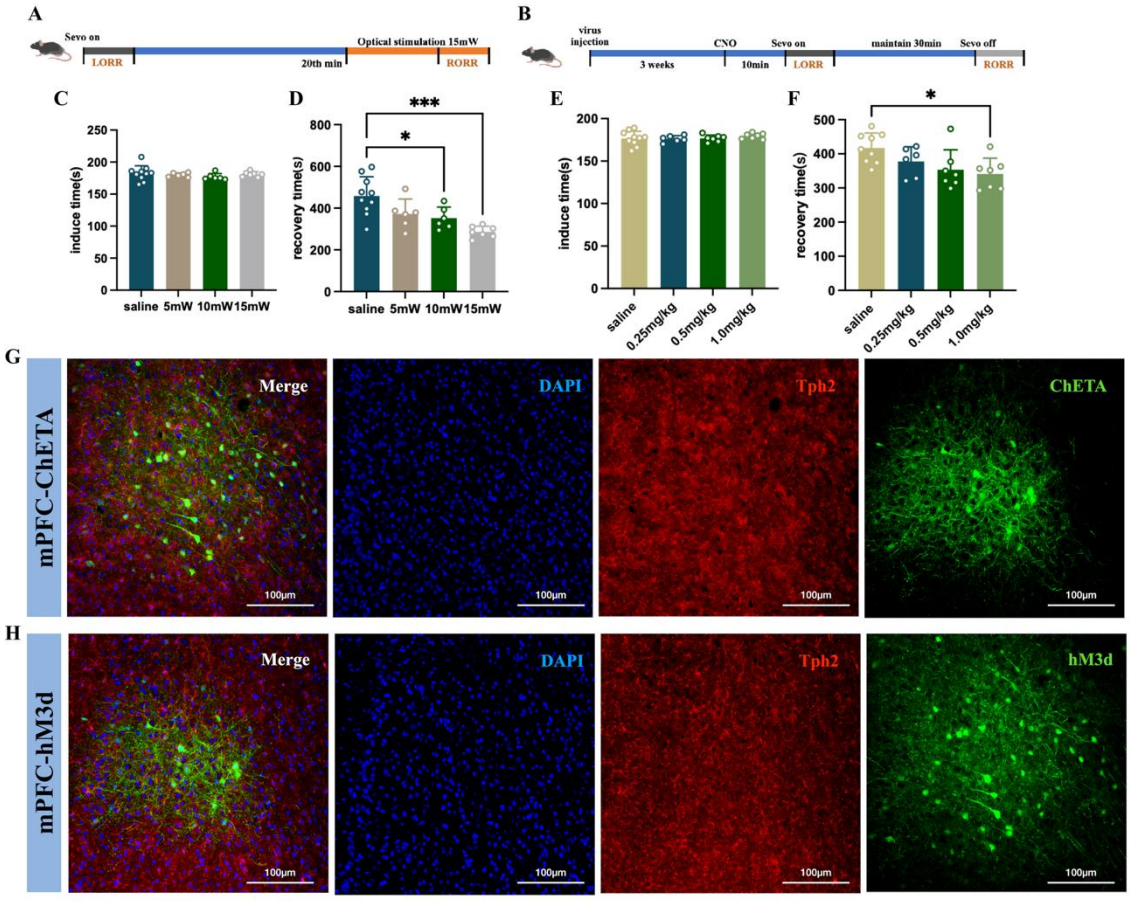

Figure S2

Figure S2. Optogenetic and chemogenetic activation of mPFC 5-HT neurons promotes arousal from sevoflurane anesthesia

(A) Experimental protocol for optogenetic stimulation of mPFC 5-HT neurons.

(B) Experimental protocol for chemogenetic stimulation of mPFC 5-HT neurons.

(C, D) Induce time and recovery time for the sham, 5mW, 10mW and 15mW groups.

(E, F) Induce time and recovery time for IP injection in saline control, 0.25 mg/kg CNO, 0.50 mg/kg CNO and 1.0 mg/kg CNO groups.

(G, H) Representative images show the co-expression of and staining for Tph2, DAPI and ChETA in the mPFC with ChETA or with hM3d.

***p<0.001, *p<0.05, Data are mean ± SEM; IP, Intraperitoneal injection; Sevo, Sevoflurane; LORR, Loss of Righting Reflex; RORR, Recovery of Righting Reflex

1 **Table S1. Summary of experimental groups of C57BL/6J mice**

Figure	Experimental groups	Number of mice
Figure 1	i.p. saline	12
	i.p. 5-HTP (25 mg/kg)	12
	i.p. 5-HTP (50 mg/kg)	12
	i.p. 5-HTP (75 mg/kg)	12
	icv. saline	6
	icv. 5-HTP (11.35 mol/l)	6
	icv. 5-HTP (22.7 mol/l)	6
	CeA saline	7
	CeA 5-HTP (2.5 mg/ml)	7
	CeA 5-HTP (5.0 mg/ml)	7
	CeA saline + mPFC saline	7
	CeA 5-HTP (5.0 mg/ml) + mPFC saline	7
	CeA 5-HTP (5.0 mg/ml) + mPFC WAY (5.0 mg/ml)	6
	CeA 5-HTP (5.0 mg/ml) + mPFC WAY (10 mg/ml)	6
Figure 2	i.p. saline	6
	i.p. 5-HTP (75 mg/kg)	6
Figure 3	i.p. saline	6
	i.p. 5-HTP (75 mg/kg)	6
Figure 5	No photostimulation	10
	Bilateral 5 mW/20 ms with photostimulation	5
	Bilateral 10 mW/20 ms with photostimulation	6
	Bilateral 15 mW/20 ms with photostimulation	10
	Left 15 mW/20 ms with photostimulation	7
	Right 15 mW/20 ms with photostimulation	6
	CeA no photostimulation + mPFC saline	10
	CeA photostimulation + mPFC saline	7
	CeA photostimulation + mPFC KET (1mg/ml)	6
	CeA photostimulation + mPFC KET (2mg/ml)	6

	CeA no photostimulation + ICV saline	10
	CeA photostimulation + ICV saline	7
	CeA photostimulation + ICV WAY (5mg/ml)	6
	CeA photostimulation + ICV WAY (10mg/ml)	6
Figure 6	i.p. saline	10
	i.p. CNO (0.25 mg/kg)	12
	i.p. CNO (0.5 mg/kg)	12
	i.p. saline	10
	i.p. CNO (0.5 mg/kg)	12
	i.p. saline + mPFC saline	10
	i.p. CNO (0.5 mg/kg) + mPFC saline	12
	i.p. CNO (0.5 mg/kg) + mPFC WAY (5mg/ml)	5
	i.p. CNO (0.5 mg/kg) + mPFC WAY (10mg/ml)	6
	i.p. CNO (0.5 mg/kg) + mPFC KET (1mg/ml)	8
	i.p. CNO (0.5 mg/kg) + mPFC KET (2mg/ml)	8
	i.p. CNO (0.5 mg/kg) + mPFC KET (4mg/ml)	6
	i.p. saline	10
	i.p. CNO (0.25 mg/kg)	12
	i.p. CNO (0.5 mg/kg)	12
Figure 7	mPFC saline	7
	mPFC 5-HTP (2.5 mg/ml)	6
	mPFC 5-HTP (5.0 mg/ml)	6
	mPFC 5-HTP (10mg/ml)	6
	mPFC no photostimulation + CeA saline	10
	mPFC photostimulation + CeA saline	7
	mPFC photostimulation + CeA WAY (5mg/ml)	6
	mPFC photostimulation + CeA KET (1mg/ml)	6
	i.p. saline + CeA saline	9
	i.p. CNO (1.0 mg/kg) + CeA saline	7
	i.p. CNO (1.0 mg/kg) + CeA KET (2mg/ml)	7

	i.p. CNO (1.0 mg/kg) + CeA KET (4mg/ml)	8
	i.p. saline	9
	i.p. CNO (1.0 mg/kg)	7
Figure S1	i.p. saline	8
	i.p. CNO (0.5 mg/kg)	8
	i.p. CNO (1.0 mg/kg)	8
Figure S2	No photostimulation	10
	5 mW/20 ms with photostimulation	6
	10 mW/20 ms with photostimulation	6
	15 mW/20 ms with photostimulation	7
	i.p. saline	9
	i.p. CNO (0.25 mg/kg)	6
	i.p. CNO (0.5 mg/kg)	7
	i.p. CNO (1.0 mg/kg)	7

1

1 **Table S2. Statistical analysis in each group**

Figure	Comparisons	Test
Figure 1	Recovery time	Ordinary one-way ANOVA
Figure 2	ΔF/F peak	Unpaired t-test
Figure 3	ΔF/F peak	Unpaired t-test
Figure 5	Recovery time	Ordinary one-way ANOVA
	Quantification of c-fos(+)/Tph2(+) section	Unpaired t-test
Figure 6	Recovery time	Ordinary one-way ANOVA
	Quantification of c-fos(+)/Tph2(+) section	Unpaired t-test
Figure 7	Recovery time	Ordinary one-way ANOVA
	Quantification of c-fos(+)/Tph2(+) section	Unpaired t-test
Figure S1	Recovery time	Ordinary one-way ANOVA
	Induce time	Ordinary one-way ANOVA
Figure S2	Recovery time	Ordinary one-way ANOVA

2

3

1 **Table S3. Reagent or resource**

Reagent or resource	Source	Identifier
Antibodies		
Mouse anti-TPH2	Sigma-Aldrich	T0678
Rabbit anti-TPH2	Novus Biologicals	NB 100-74555
Rabbit anti-c-fos	Cell Signaling Technology	2250T
Alexa Fluor 546 anti-mouse IgG	Thermo Fisher Scientific	A10036
Alexa Fluor cy5 anti-rabbit IgG	Thermo Fisher Scientific	A10523
Bacterial and virus strains		
pAAV-TPH2 PRO-ChETA-EYFP-WPRES-PAS	Shengbo, Co., Ltd.	N/A
rAAV-TPH2-hM3D(Gq)-EGFP-WPRE	Brain VTA Technology Co., Ltd.	N/A
rAAV-TPH2-hM4D(Gi)-mCherry-WPREs	Brain VTA Technology Co., Ltd.	N/A
rAAV-TPH2-GCaMP6S-WPRE-hGH-pA	Brain VTA Technology Co., Ltd.	N/A
rAAV-EF1a-DIO-mCherry-F2A-TVA-WPRE-hGE polyA	Brain VTA Technology Co., Ltd.	N/A
rAAV-EF1α-DIO-oRVG-WPRE-hGE polyA	Brain VTA Technology Co., Ltd.	N/A
rAAV-TPH2-CRE-WPRE-hGE polyA	Brain VTA Technology Co., Ltd.	N/A
RV-EnvA-ΔG-EGFP	Brain VTA Technology Co., Ltd.	N/A
Chemicals, peptides, and recombinant proteins		
sevoflurane	Maruishi Pharmaceutical Co., Ltd.	H20150020
5-HTP	Sigma-Aldrich	H9772
WAY-100635	Sigma-Aldrich	W108
KET	Sigma-Aldrich	S006
Clozapine N-oxide (CNO)	Brain VTA Technology Co., Ltd.	CNO
CTB-555	Brain VTA Technology Co., Ltd.	N/A
Experimental models: Organisms/strains		
C57BL/6J mice	the Animal Center of Zhejiang University School of Medicine	N/A

Software and algorithms

Fiber photometry system	Inper	C11946
ImageJ	NIH, Bethesda, MD, USA	https://imagej.nih.gov/ij/
GraphPad Prism 8.0		
SPSS version 26.0		

1

1